Article

# Zirconium Sandwich Complexes with η³ Indenyl Ligands: Well-Defined Precursors for Zirconocene-Mediated Coupling Reactions

Christopher A. Bradley, Ivan Keresztes, Emil Lobkovsky, Victor G. Young, and Paul J. Chirik

*J. Am. Chem. Soc.*, **2004**, 126 (51), 16937-16950• DOI: 10.1021/ja045072v • Publication Date (Web): 03 December 2004



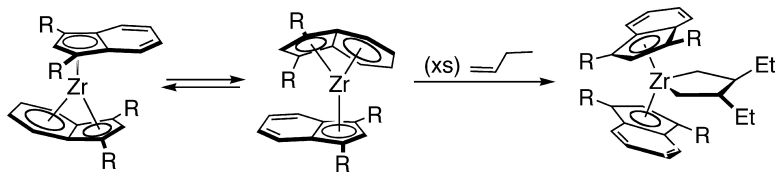


## More About This Article

Additional resources and features associated with this article are available within the HTML version:

- Supporting Information
- Links to the 10 articles that cite this article, as of the time of this article download
- Access to high resolution figures
- Links to articles and content related to this article
- Copyright permission to reproduce figures and/or text from this article

View the Full Text HTML

J|A|C|S
ARTICLES
Published on Web 12/03/2004

# Zirconium Sandwich Complexes with $\eta^9$ Indenyl Ligands: Well-Defined Precursors for Zirconocene-Mediated Coupling Reactions

Christopher A. Bradley,[†] Ivan Keresztes,[†] Emil Lobkovsky,[†] Victor G. Young,[‡] and Paul J. Chirik*,[†]

*Contribution from the Department of Chemistry and Chemical Biology, Baker Laboratory, Cornell University, Ithaca, New York 14853, and Department of Chemistry, University of Minnesota, Minneapolis, Minnesota 55455*

Received August 16, 2004; E-mail: pc92@cornell.edu

***Abstract:*** A family of isolable, well-defined bis-indenyl zirconium sandwich complexes, ($\eta^5$-$C_9H_5$-1,3-$R_2$)($\eta^9$-$C_9H_5$-1,3-$R_2$)Zr (R = silyl, alkyl), have been prepared by either alkane reductive elimination or alkali metal reduction of a suitable zirconium(IV) dihalide precursor. Crystallographic characterization of two of these derivatives, R = $SiMe_2CMe_3$ and $CHMe_2$, reveals unprecedented $\eta^9$ coordination of one of the indenyl ligands. Variable-temperature and EXSY NMR studies establish that the $\eta^5$ and $\eta^9$ rings are rapidly interconverting in solution. The sandwich complexes serve as effective sources of low-valent zirconium reacting rapidly with both olefins and alkynes at ambient temperature. In contrast to bis-cyclopentadienyl chemistry, the olefin adducts of the bis-indenyl zirconium sandwiches undergo preferential C−H activation to yield the corresponding allyl hydride compounds, although reaction with excess olefin proceeds through the $\eta^2$-olefin adduct, forming the corresponding zirconacyclopentane.

## Introduction

Transition metal sandwich compounds, more commonly referred to as metallocenes, occupy a central role, both historically and practically, in organotransition metal chemistry.[1] Specifically, group 4 metal sandwich complexes are of long-standing interest given their indispensable role in organic coupling reactions[2] and small molecule activation processes.[3] Despite this utility, there is a paucity of isolable or even spectroscopically characterized low-valent group 4 transition metal sandwich complexes. Attempts to prepare [($\eta^5$-$C_5H_5$)$_2$-Ti] by either direct synthesis[4] or reduction of a suitable halide precursor leads to the bridging titanium fulvalene hydride [($\eta^5$-$C_5H_5$)Ti]$_2$($\mu$,$\eta^5$-$C_{10}H_8$)($\mu$-H)$_2$, arising from activation of cyclopentadienyl C−H bonds.[5,6] However, the putative titanium sandwich can be trapped using a sufficiently $\pi$-accepting ligand such as a phosphine,[7] alkyne,[8] carbon monoxide,[9] or dinitrogen.[10] Introduction of methyl groups onto the cyclopentadienyl ligand provides steric protection of the titanium center, allowing observation of the titanium sandwich, [($\eta^5$-$C_5Me_5$)$_2$Ti].[11] This molecule is quite reactive, promoting activation of dinitrogen to form [($\eta^5$-$C_5Me_5$)$_2$Ti]$_2$($\mu_2$,$\eta^1$,$\eta^1$-$N_2$) as well as participating in competitive cyclometalation of the cyclopentadienyl methyl groups to yield ($\eta^5$-$C_5Me_5$)($\eta^5$-$C_5Me_4$-$\eta^1$-$CH_2$)TiH.[12] Likewise, our laboratory has observed a transient, silylated titanium sandwich ($\eta^5$-$C_5H_3$-1,3-($SiMe_3$)$_2$)$_2$Ti that reacts rapidly with $N_2$ to afford the end-on dinitrogen complex [($\eta^5$-$C_5H_3$-1,3-($SiMe_3$)$_2$)$_2$-Ti]$_2$($\mu_2$,$\eta^1$,$\eta^1$-$N_2$).[13] This molecule serves as a useful synthon for the preparation of monomeric imido complexes that participate in nitrene group transfer processes.

Crystallographic characterization of an isolable titanium sandwich ($\eta^5$-$C_5Me_4SiMe_2CMe_3$)$_2$Ti was recently achieved by Lawless by reduction of the corresponding titanium(III) monochloride.[14] Independently, Mach and co-workers prepared several other related examples of the general form ($\eta^5$-$C_5Me_4R$)$_2$Ti (R = $SiMe_3$, $SiMe_2Ph$, $SiMePh_2$, $SiMe_2CH_2CH_2Ph$).[15,16] In-situ

[†] Cornell University.
[‡] University of Minnesota.

(1) For leading reviews on metallocene chemistry, see: *The Metallocenes: Synthesis, Reactivity and Applications;* Togni, A., Halterman, R. L., Eds.; Wiley-VCH: Weinheim, 1998.
(2) (a) Negishi, E.-I.; Takahashi, T. *Acc. Chem. Res.* **1994**, *27*, 124. (b) Rosenthal, U.; Pellny, P.-M.; Kirchbauer, F. G.; Burlakov, V. V. *Acc. Chem. Res.* **2000**, *33*, 119.
(3) (a) Fryzuk, M. D. *Chem. Rec.* **2003**, *3*, 2. (b) Fryzuk, M. D.; Johnson, S. A. *Coord. Chem. Rev.* **2000**, *200*, 379.
(4) Fischer, A. K.; Wilkinson, G. *J. Inorg. Nucl. Chem.* **1956**, *2*, 149.
(5) Brintzinger, H. H.; Bercaw, J. E. *J. Am. Chem. Soc.* **1970**, *92*, 6182.
(6) Troyanov, S. I.; Antropiusova, H.; Mach, K. *J. Organomet. Chem.* **1992**, *427*, 49.
(7) (a) $PF_3$: Sikora, D. J.; Rausch, M. D.; Rogers, R. D.; Atwood, J. L. *J. Am. Chem. Soc.* **1981**, *103*, 1265. (b) $PMe_3$: Kool, L. B.; Rausch, M. D.; Alt, H. G.; Herberhold, M.; Thewalt, U.; Honold, B. *J. Organomet. Chem.* **1986**, *310*, 27. (c) $Me_2PCH_2CH_2PMe_2$: Girolami, G. S.; Wilkinson, G.; Thortonpett, M.; Hursthouse, M. B. *J. Chem. Soc., Dalton Trans.* **1984**, 2347.
(8) Rosenthal, U.; Burlakov, V. V.; Arndt, P.; Baumann, W.; Spannenberg, A. *Organometallics* **2003**, *22*, 884.
(9) Sikora, D. J.; Macomber, D. W.; Rausch, M. D. *Adv. Organomet. Chem.* **1986**, *25*, 317.
(10) Berry, D. H.; Procopio, L. J.; Carroll, P. J. *Organometallics* **1988**, *7*, 570.
(11) Bercaw, J. E.; Brintzinger, H. H. *J. Am. Chem. Soc.* **1971**, *93*, 2045.
(12) Bercaw, J. E. *J. Am. Chem. Soc.* **1974**, *96*, 5087.
(13) Hanna, T. E.; Keresztes, I.; Lobkovsky, E.; Bernskoetter, W. H.; Chirik, P. J. *Organometallics* **2004**, *23*, 3448.
(14) Hitchcock, P. B.; Kerton, F.; Lawless, G. A. *J. Am. Chem. Soc.* **1998**, *120*, 10264.
(15) Lukesová, L.; Horácek, M.; Stepnicka, P.; Fejfarová, K.; Gyepes, R.; Cisorová, I.; Kubista, J.; Mach, K. *J. Organomet. Chem.* **2002**, *663*, 134.
(16) Horácek, M.; Kupfer, V.; Thewalt, U.; Stepnicka, P.; Polásek, M.; Mach, K. *Organometallics* **1999**, *18*, 3572.

infrared spectroscopic studies recently conducted in our laboratory have shown that these molecules coordinate two equivalents of $N_2$ at low temperature, forming monomeric titanium bis-dinitrogen complexes that are isoelectronic and isostructural with more familiar dicarbonyl derivatives.[17]

Sandwich complexes of zirconium and hafnium are expected to be more challenging to synthesize owing to the greater thermodynamic potential for these metals to attain their highest oxidation state. While a bis-cyclopentadienyl zirconium complex [($\eta^5$-$C_5H_5$)$_2$Zr$^{II}$] has not been isolated or even experimentally demonstrated, Negishi[18] developed a practical route to a functional equivalent of the molecule by addition of two equivalents of *n*-BuLi to zirconocene dichloride at low temperature. Detailed spectroscopic studies on the in-situ-generated "zirconocene" reagent revealed a complex mixture of Zr(III) and Zr(IV) compounds rather than a discrete zirconium(II) sandwich.[19] Nonetheless, this procedure is effective for the coupling of numerous unsaturated organic molecules[20] and has found widespread utility in organic synthesis[21] and materials chemistry.[22] Attempts to protect the zirconium center with substituted cyclopentadienyl ligands produces more well-defined chemistry, although observation of a sandwich has not been realized. For example, reduction of ($\eta^5$-$C_5Me_5$)$_2$ZrCl$_2$ with sodium amalgam induces dinitrogen activation to form the end-on dinitrogen complex [($\eta^5$-$C_5Me_5$)$_2$Zr($\eta^1$-N$_2$)]$_2$($\mu_2$,$\eta^1$,$\eta^1$-N$_2$).[23] Analogous chemistry was also observed with the corresponding permethylhafnocene.[24]

Attempts to prepare zirconium sandwich complexes have also resulted in intramolecular C−H activation of cyclopentadienyl substituents. Reduction of ($\eta^5$-$C_5Me_4SiMe_3$)$_2$ZrCl$_2$ with Mg at elevated temperature affords a mixture of products, one of which has been identified as the cyclometalated zirconocene hydride, ($\eta^5$-$C_5Me_4SiMe_3$)($\eta^5$-$C_5Me_4$-$\eta^1$-$SiMe_2CH_2$)ZrH.[25] This product is postulated to arise from oxidative addition of a [SiMe$_3$] C−H bond to a transient zirconium(II) sandwich. Our laboratory has been studying the chemistry of low-valent silylated bis-cyclopentadienyl zirconium(IV) compounds and discovered that alkane reductive elimination may be used to prepare the reactive cyclometalated hydride ($\eta^5$-$C_5H_3$-1,3-(SiMe$_3$)$_2$)($\eta^5$-$C_5H_3$-$\eta^1$-1-$SiMe_2CH_2$-3-SiMe$_3$)ZrH.[26] This complex, when exposed to 1 atm of dinitrogen, forms the side-on-bound dinitrogen complex [($\eta^5$-$C_5H_3$-1,3-(SiMe$_3$)$_2$)$_2$Zr]$_2$($\mu_2$,$\eta^2$,$\eta^2$-N$_2$).[26]

Provided these results, we became interested in studying both the mechanism and products of alkane reductive elimination from the corresponding bis-indenyl zirconocene alkyl hydrides. The indenyl anion, $C_9H_7^-$, is related to the ubiquitous cyclopentadienyl ligand with the potential to coordinate to a transition metal as a monoanionic, five-electron, $L_2X$-type ligand.[27] However, most indenyl complexes show distinct $\eta^3$,$\eta^2$ coordination, where two of the five metal−carbon bonds are significantly longer than the other three.[28] Replacement of cyclopentadienyl with indenyl ligands often leads to enhanced or unique reactivity.[29] This behavior, termed the "indenyl effect", is most frequently observed in associative substitution reactions, where indenyl complexes undergo faster ligand exchange as a result of the indenyl ring slippage from $\eta^5$ to $\eta^3$ coordination.[30]

Indenyl anions are common ancillary ligands in group 4 metallocene chemistry, owing to their role in stereospecific olefin polymerization[31] and catalytic bond-forming reactions.[32] In some cases, enhanced catalytic activity is observed for the indenyl complex as compared to the cyclopentadienyl compound.[33] We recently communicated the effect of indenyl ligand substitution on the outcome of alkane reductive elimination from group 4 metallocene alkyl hydride complexes. Specifically, we discovered that the silylated bis-indenyl zirconocene isobutyl hydride ($\eta^5$-$C_9H_5$-1,3-(SiMe$_3$)$_2$)$_2$Zr($CH_2CHMe_2$)H undergoes facile extrusion of isobutane at ambient temperature to yield the zirconium sandwich complex ($\eta^5$-$C_9H_5$-1,3-(SiMe$_3$)$_2$)-($\eta^9$-$C_9H_5$-1,3-(SiMe$_3$)$_2$)Zr and crystallographically characterized its $\eta^5$,$\eta^6$-bis(indenyl)zirconium−THF adduct.[34] Here we describe a detailed study of bis-indenyl zirconium complexes including complete solution spectroscopic and solid-state characterization. X-ray crystallographic studies on two examples have established an unprecedented $\eta^9$ indenyl−metal interaction that masks the formally low-valent zirconium center. This family of molecules promotes carbon−carbon bond-forming reactions with olefins and alkynes, providing isolable, well-characterized species for "zirconocene"-mediated coupling reactions.

## Results and Discussion

**Synthesis and Observation of Bis-indenyl Zirconium Isobutyl Hydride Complexes.** We recently reported both the steric and electronic properties of a family of disubstituted indenyl ligands by evaluation of the structural and spectroscopic properties of the resulting zirconocene dichloride and dicarbonyl compounds in addition to the related iron(II) sandwiches.[35] In agreement with the trend established in cyclopentadienyl chemistry,[26] silylated indenes impart more electrophilic zirco-


(17) Hanna, T. E.; Lobkovsky, E.; Chirik, P. J. *J. Am. Chem. Soc.* **2004**, *126*, 14688.
(18) Negishi, E.-I.; Cederbaum, F. E.; Takahashi, T. *Tetrahedron Lett.* **1986**, *27*, 2829.
(19) Dioumaev, V. K.; Harrod, J. F. *Organometallics* **1997**, *16*, 1452.
(20) Watt, G. W.; Drummond, F. O. *J. Am. Chem. Soc.* **1970**, *92*, 826.
(21) For recent examples, see: (a) Chinkov, N.; Majumdar, S.; Marek, I. *J. Am. Chem. Soc.* **2003**, *125*, 13258. (b) Urabe, H.; Suzuki, D.; Sasaki, M.; Sato, F. *J. Am. Chem. Soc.* **2003**, *125*, 4036. (c) Paquette, L. A.; Kim, I. H.; Cuniere, N. *Org. Lett.* **2003**, *5*, 221. (d) Takahashi, T.; Li, Y.; Ito, T.; Xu, F.; Nakajima, K.; Liu, Y. *J. Am. Chem. Soc.* **2002**, *124*, 1144.
(22) (a) Johnson, S. A.; Liu, F.-Q.; Suh, M. C.; Zürcher, S.; Haufe, M.; Mao, S. S. H.; Tilley, T. D. *J. Am. Chem. Soc.* **2003**, *125*, 4199. (b) Lucht, B. L.; Buretea, M. A.; Tilley, T. D. *Organometallics* **2000**, *19*, 3469. (c) Takahashi, T.; Kotora, M.; Hara, R.; Xi, Z. *Bull. Chem. Soc. Jpn.* **1999**, *72*, 2591. (d) Lucht, B. L.; Mao, S. S. H.; Tilley, T. D. *J. Am. Chem. Soc.* **1998**, *120*, 4354.
(23) Manriquez, J. M.; Bercaw, J. E. *J. Am. Chem. Soc.* **1974**, *96*, 6229.
(24) Roddick, D. M.; Fryzuk, M. D.; Seidler, P. F.; Hillhouse, G. L.; Bercaw, J. E. *Organometallics* **1985**, *4*, 97.
(25) Horácek, M.; Stepnicka, P.; Kubista, J.; Fejfarova, K.; Gyepes, R.; Mach, K. *Organometallics* **2003**, *22*, 861.
(26) Pool, J. A.; Lobkovsky, E.; Chirik, P. J. *J. Am. Chem. Soc.* **2003**, *125*, 2241.
(27) For a discussion of this nomenclature, see: Crabtree, R. H. *The Organometallic Chemistry of the Transition Metals*, 2nd ed.; John Wiley: New York, 1994; pp 24−38.
(28) (a) Calhorda, M. J.; Verios, L. F. *Comm. Inorg. Chem.* **2001**, *22*, 375. (b) Zargarian, D. *Coord. Chem. Rev.* **2002**, *233*−*234*, 157. (c) Trnka, T. M.; Bonanno, J. B.; Bridgewater, B. M.; Parkin, G. *Organometallics* **2001**, *20*, 3255.
(29) (a) Calhorda, M. J.; Romao, C. C.; Verios, L. F. *Chem. Eur. J.* **2002**, *8*, 868. (b) Marder, R. B.; Roe, D. C.; Milstein, D. *Organometallics* **1988**, *7*, 1451.
(30) (a) Rerek, M. E.; Basolo, F. *J. Am. Chem. Soc.* **1984**, *106*, 5908. (b) Kakkar, A. K.; Taylor, N. J.; Marder, T. J.; Shen, N.; Hallinan, N.; Basolo, F. *Inorg. Chim. Acta* **1992**, *198*−*200*, 219. (c) Wescott, S. A.; Kakkar, A. K.; Stringer, G.; Taylor, N. J.; Marder, T. B. *J. Organomet. Chem.* **1990**, *394*, 777.
(31) Coates, G. W. *Chem. Rev.* **2000**, *100*, 1223.
(32) Hoveyda, A. H.; Morken, J. P. In *The Metallocenes: Synthesis, Reactivity and Applications*; Togni, A., Haltermann, R. L., Eds.; Wiley-VCH: Weinheim, 1998; Vol. 2, Chapter 8.
(33) Okuda, J.; König, P.; Rushkin, I. L.; Kang, H.-C.; Massa, W. *J. Organomet. Chem.* **1995**, *501*, 37.
(34) Bradley, C. A.; Lobkovsky, E.; Chirik, P. J. *J. Am. Chem. Soc.* **2003**, *125*, 8810.
(35) Bradley, C. A.; Flores-Torres, S.; Lobkovsky, E.; Abruña, H. D.; Chirik, P. J. *Organometallics* **2004**, *23*, 5332.

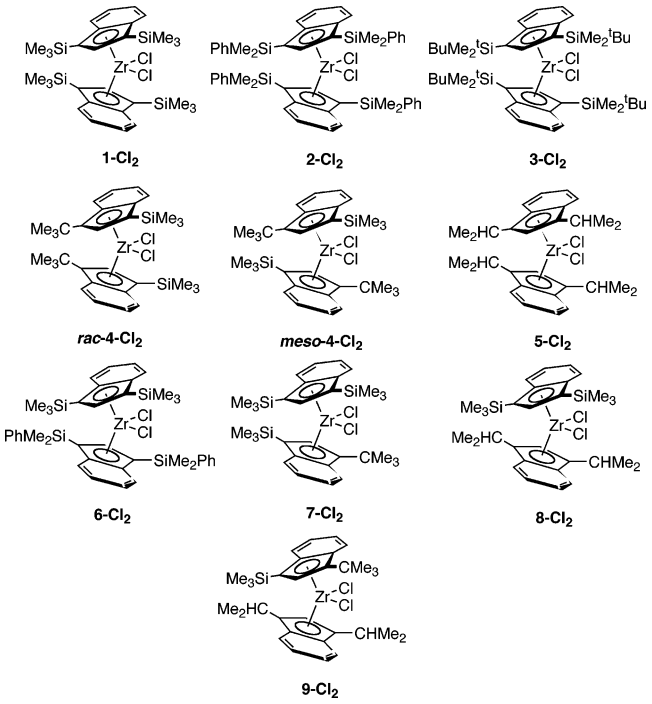


***Figure 1.*** Zirconocene dichloride precursors and their shorthand designations.

nium centers than their alkylated counterparts. This family of zirconocene dichloride complexes serves as the foundation for the present study (Figure 1). As we noted in our prior report,[35] the zirconocene dichloride **4-Cl$_2$** was isolated as a near equimolar mixture of *rac* and *meso* diastereomers that were not separated for subsequent experiments. In this study, we also included two new "mixed-ring" zirconocene dichlorides **8-Cl$_2$** and **9-Cl$_2$** (Figure 1).

Synthesis of the desired zirconocene isobutyl hydride complexes was accomplished by addition of two equivalents of isobutyllithium to the corresponding zirconocene dichloride (eq 1). Attempts to alkylate **1-Cl$_2$** with two equivalents of *tert*-

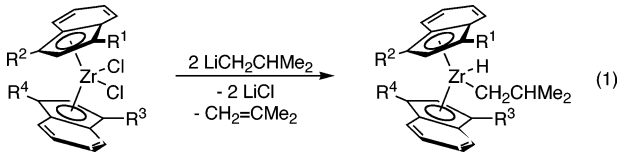


(1)

butyllithium[26,36] produced an intractable mixture of products. While definitive mechanistic data has not been obtained, isobutyl hydride formation with $LiCH_2CHMe_2$ most likely proceeds by initial hydride transfer to the zirconium liberating isobutene, followed by alkylation of the intermediate zirconocene hydrido chloride. The olefin byproduct was detected and quantified by a combination of $^1$H NMR spectroscopy and GC-MS experiments. Initial alkylation to form a zirconocene isobutyl chloride followed by $\beta$-hydrogen elimination is unlikely as preparation of **1-(CH$_2$CHMe$_2$)Cl** has been accomplished and subsequent $\beta$-hydrogen elimination was not observed. These results are in agreement with previous studies of bis-cyclopentadienyl zirconium primary alkyl chloride complexes that are resistant to $\beta$-hydrogen elimination, most likely due to important contributions from a resonance structure where the chloride acts as a $\pi$-donor, coordinatively saturating the zirconium center.[37]

Treatment of the other zirconocene dichloride complexes with isobutyllithium yielded analogous chemistry. Alkylation of the mixture of *rac* and *meso* diastereomers of **4-Cl$_2$** produced three isomeric isobutyl hydride complexes in approximately equal amounts. Two of the isomers arise from the two distinct *meso*-zirconocene isobutyl hydrides, while the other derives from the one possible isomer of the *rac* compound. In the case of **7-Cl$_2$**, reaction with two equivalents of isobutyllithium afforded a 70:30 mixture of isomeric isobutyl hydrides.

Each of the bis-indenyl zirconocene isobutyl hydrides undergoes reductive elimination of isobutane at ambient temperature (vide infra). Consistent with the electron-donating properties of alkyl substituents and cooperative steric effects,[26] the isopropyl-substituted compound, **5-(CH$_2$CHMe$_2$)H**, undergoes the slowest reductive elimination in the series, allowing observation of the isobutyl hydride for several hours at 22 °C. In contrast, the silylated zirconocene isobutyl hydride complexes undergo rapid reductive elimination, most likely a result of electronic destabilization of the Zr(IV) ground state.[38] Despite the complications arising from swift reductive elimination, most of the zirconocene isobutyl hydrides have been characterized in situ by NMR spectroscopy. Each alkyl hydride was generated in near quantitative yield and exhibited either $C_s$ or $C_1$ symmetry, depending on the indenyl substitution pattern. Moreover, each spectrum contained diagnostic upfield resonances in the vicinity of 0 ppm assigned to the diastereotopic protons on the methylene carbon bound to the zirconium (see Experimental Section and Supporting Information).

**Synthesis of Homoleptic Bis-indenyl Zirconium Sandwich Complexes.** As we previously communicated,[34] reductive elimination of isobutane from **1-(CH$_2$CHMe$_2$)H** proceeds rapidly at 22 °C and affords a burgundy complex, **1** (eq 2). A

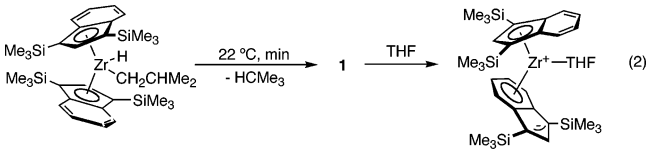


(2)

combination of elemental analysis, solution molecular weight determinations, and reactivity studies with HCl, CO and alkynes established the empirical formula of the molecule as $(C_9H_5$-1,3-$(SiMe_3)_2)_2Zr$, consistent with the bis-indenyl zirconium sandwich complex. However, both $^1$H and $^{13}$C NMR spectroscopy indicated a molecule of $C_s$ symmetry with inequivalent indenyl ligands rather than the $C_{2v}$-symmetric zirconium sandwich with $\eta^5,\eta^5$-indenyl rings. While structural elucidation of **1** was frustrated by poor crystal quality, addition of THF afforded large red blocks suitable for X-ray diffraction. The molecular structure established the identity of the complex as $(\eta^5$-$C_9H_5$-1,3-$(SiMe_3)_2)(\eta^6$-$C_9H_5$-1,3-$(SiMe_3)_2)Zr$(THF) (**1-THF**), where one of the indenyl ligands had undergone net haptotropic rearrangement.[39,40] Importantly, the NMR spectra of **1** and

(36) Pool, J. A.; Bradley, C. A.; Chirik, P. J. *Organometallics* **2002**, *21*, 1271.
(37) Chirik, P. J.; Day, M. W.; Labinger, J. A.; Bercaw. J. E. *J. Am. Chem. Soc.* **1999**, *121*, 10308.
(38) Pool, J. A.; Lobkovsky, E.; Chirik, P. J. *Organometallics* **2003**, *22*, 2797.
(39) Albright, T. A.; Hofmann, P.; Hoffmann, R.; Lillya, C. P.; Dobosh, P. A. *J. Am. Chem. Soc.* **1983**, *105*, 3396.
(40) Opruneko, Y. F.; Akhmedov, N. G.; Laikov, D. N.; Malyugina, S. G.; Mstislavsky, V. I.; Roznyatovsky, V. A.; Ustynyuk, Y. A.; Utsynyuk, N. A. *J. Organomet. Chem.* **1999**, *583*, 136.

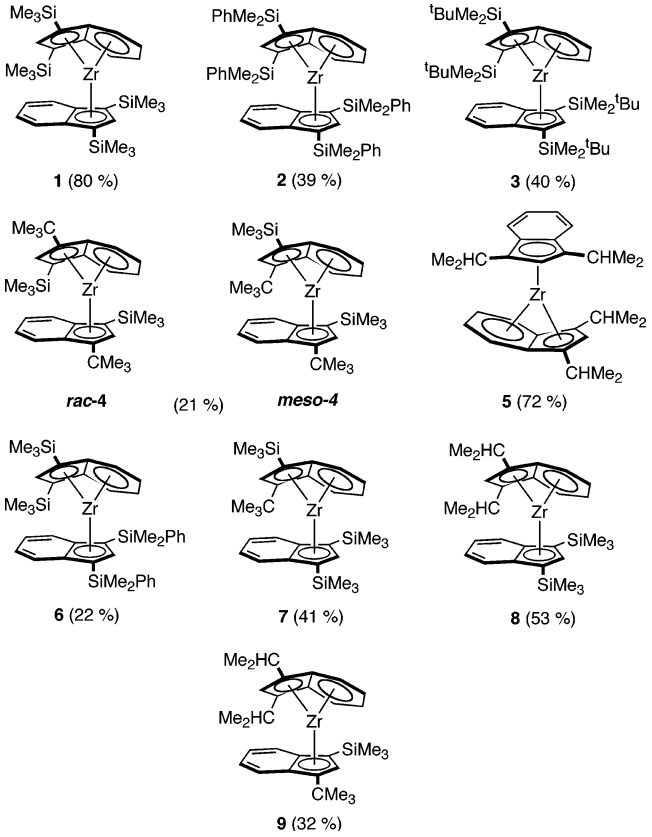


***Figure 2.*** Labeling scheme and isolated yield for the bis-indenyl zirconium sandwich complexes.

**1-THF** were similar, leading to the conclusion that **1** was the formally zwitterionic zirconium sandwich ($\eta^5$-$C_9H_5$-1,3-$(SiMe_3)_2$)-($\eta^6$-$C_9H_5$-1,3-$(SiMe_3)_2$)Zr. As will be described in a later section, newly acquired X-ray crystallographic data on related zirconium sandwiches has established unprecedented $\eta^9$ hapticity of one of the indenyl ligands, indicating that the structure of **1** is in fact ($\eta^5$-$C_9H_5$-1,3-$(SiMe_3)_2$)($\eta^9$-$C_9H_5$-1,3-$(SiMe_3)_2$)Zr.

Reductive elimination from the other homoleptic bis-indenyl zirconocene isobutyl hydrides, **2-($CH_2CHMe_2$)H**, **3-($CH_2$-$CHMe_2$)H**, ***rac*/*meso*-4-($CH_2CHMe_2$)H**, and **5-($CH_2CHMe_2$)-H**, produced similar products. In each case, the analytical and NMR spectroscopic data (vide infra) are consistent with the formation of the bis-indenyl zirconium sandwich complex (Figure 2). Each compound was isolated as a burgundy solid in moderate yield. Monitoring the isobutane reductive elimination reactions in situ by NMR spectroscopy revealed that each sandwich compound is formed in near quantitative yield, demonstrating that the low isolated yields are a consequence of the high lipophilicity of the molecules. The bis-indenyl zirconium sandwich complexes can also be prepared by alkali metal reduction of the dichloride precursor (eq 3). Although in most cases alkane reductive elimination is the preferred method, synthesis of **5** is best achieved by reduction of **5-$Cl_2$** with sodium amalgam due to a secondary reaction of the resulting sandwich with the isobutene byproduct (vide infra).

**Crystallographic Characterization of 3 and 5 and Electronic Structure.** Two of the bis-indenyl zirconium sandwich complexes have been characterized by X-ray crystallography. Cooling a saturated pentane solution of **3** to −35 °C afforded burgundy blocks suitable for diffraction. The compound crystallizes with two independent molecules in the asymmetric unit,

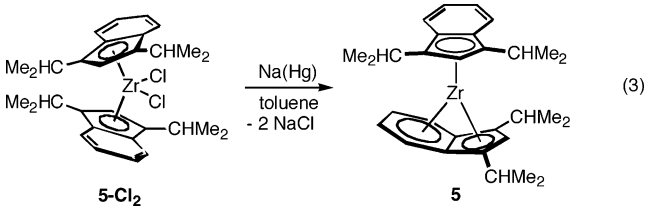


(3)

one of which is presented in Figure 3. The other molecule (Supporting Information) is positionally disordered and was successfully modeled with two independent molecules, with an 87:13 occupancy of the two sites. The disorder is such that a 180° rotation along the common coaxial direction of the two indenyl ligands brings all atoms, except the zirconium and four carbons, into complete overlap. A similar recrystallization procedure was used to obtain single crystals of **5**. The solid-state structure of this sandwich complex is presented in Figure 4.

The solid-state structures of both **3** and **5** established the identity of the molecules as the bis-indenyl zirconium sandwich complexes where one of the rings is engaged in an $\eta^9$ interaction with the zirconium. Selected bond distances and angles for both compounds are presented in Table 1. While the hapticity of the indenyl ligands in **3** and **5** are similar, the ring orientations are significantly different. In the more sterically hindered sandwich **3** the indenyl rings are staggered with a rotational angle of 177.8(4)°. This conformation contrasts the eclipsed geometry observed in the corresponding zirconium dicarbonyl complex.[35] In the solid-state structure of **5**, the ligands adopt a near gauche arrangement with a rotational angle of 84.6(2)°, in analogy to the solid-state orientations of most of the bis-indenyl zirconium dichloride precursors.[35] In both cases, the substituents orient such that the large groups point away from the interior of the sandwich. For **3**, the Si-$^t$Bu groups are directed above and below the planes of the rings, while in **5**, the isopropyl methine hydrogens are pointed "in" toward the zirconium. Though the conformations of these two sandwiches appear to minimize transannular steric interactions of the indenyl substituents, the role of crystal packing effects and kinetic preferences associated with crystallization cannot be excluded. As expected for a metal sandwich complex, the angle between the centroid of the $\eta^5$ and the centroid to the midpoint of the two bridging carbons on the $\eta^9$ ligand approaches 180°. For **3**, this angle deviates only 0.8(2)° from linearity, while a more pronounced bend of 6.2(2)° is observed for **5**.

As can be seen from the data compiled in Table 1, the zirconium−carbon distances for the six-membered ring of the $\eta^9$ indenyl ligand in both **3** and **5** range between 2.255 and 2.520 Å, within the range typically ascribed to zirconium−carbon bonds in $\pi$-complexed ligands. For comparison, the corresponding distances to the six-membered ring on the $\eta^5$ ligand range between 3.416 and 4.185 Å, outside the range of a bonding interaction. Coordination of the benzo portion of the $\eta^9$ indenyl ligand breaks the planarity of the ring and shortens the bonds between the zirconium and the bridgehead carbon atoms. The planes of the five- and six-membered rings on the $\eta^9$ ligand are buckled by 37.1(3)° and 37.6(1)° in **3** and **5**, respectively. Likewise, the centroids of the five- and six-membered rings form angles of 60.7(6)° and 61.3(4)° with the zirconium center. Relatively short Zr−C(7) and Zr−C(8) distances of 2.264(4) and 2.270(3) Å are observed for **3**, while comparable distances

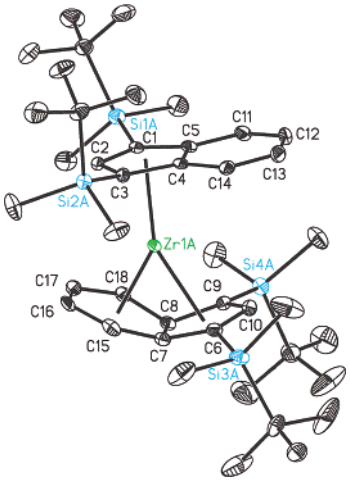


***Figure 3.*** Molecular structure of one of the independent molecules of **3** at 30% probability ellipsoids. Hydrogen atoms omitted for clarity.

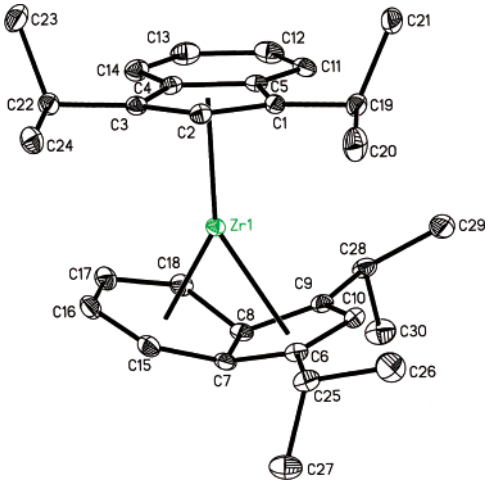


***Figure 4.*** Molecular structure of **5** at 30% probability ellipsoids. Hydrogen atoms omitted for clarity.

of 2.267(2) and 2.255(2) Å are present in **5**. For reference, more typical zirconium−carbon bond distances in the range from 2.539(2) to 2.561(4) Å are observed for C(4) and C(5) in the $\eta^5$ ligand. Moreover, the coordinated six-membered rings are slightly buckled by 4.9(2)° and 6.2(2)° in **3** and **5**, respectively, less than the buckling of 19° observed in **1-THF,**[34] suggesting that the aromaticity of the benzo ring is preserved upon coordination to zirconium. Similar observations have been made by Basolo in compounds where an $\eta^5$ indenyl ligand "slips" to $\eta^3$ hapticity.[30b] These results, coupled with the structures of **3** and **5**, underscore the flexibility of the indenyl $\pi$-system to accommodate the coordination requirements of the metal.

The carbon−carbon bond distances in the six-membered rings also lengthen somewhat upon coordination to the zirconium. For the $\eta^9$ indenyl ring in **3**, the C(17)−C(18) and C(15)−C(16) distances are 1.402(6) and 1.406(6) Å, respectively, slightly elongated from the corresponding C(11)−C(12) and C(13)−C(14) bond lengths of 1.350(6) and 1.366(6) Å in the $\eta^5$ ligand. A similar effect is also observed in **5**, where the C(17)−C(18) and C(15)−C(16) distances are 1.426(3) and 1.418(3) Å, respectively, while C(11)−C(12) and C(13)−C(14) are 1.369(2) and 1.367(3) Å.

Because the indenyl anion is a 10 $\pi$-electron system, it is isoelectronic with cyclooctatetrenyl dianion[41] and its transannularly bridged analogue pentalene, $C_8H_6^{2-}$.[42] On the basis of this relationship, indenyl ligands would be expected to engage in bonding to transition metals with hapticities ranging from $\eta^1$ to $\eta^9$. Transition metal−indenyl bonding is usually confined to direct interactions with the five-membered ring, although it is well known that this class of ligand frequently "slips" from $\eta^5$ to $\eta^3$ coordination as a result of a gain in aromaticity within the benzo ring.[30] Examples of $\eta^6$-indene, $C_9H_8$, complexes are known, but in these cases the cyclopentadienyl ligand is protonated in analogy to well-known transition metal arene complexes.[43a,b] In addition, examples of heterobimetallic $\eta^6,\eta^5$ complexes where indenyl acts as a bridging ligand have also been reported.[43c]

***Table 1.*** Comparison of the Bond Distances (Å) and Angles (deg) of the $\eta^5$ and $\eta^9$ Indenyl Ligands in **3** and **5**

| $\eta^5$ indenyl | | | $\eta^9$ indenyl | | |
|---|---|---|---|---|---|
| | **3** | **5** | | **3** | **5** |
| Zr−C(1) | 2.513(3) | 2.485(2) | Zr−C(9) | 2.612(3) | 2.574(2) |
| Zr−C(2) | 2.455(3) | 2.517(2) | Zr−C(10) | 2.752(3) | 2.784(2) |
| Zr−C(3) | 2.496(3) | 2.536(2) | Zr−C(6) | 2.618(3) | 2.626(2) |
| Zr−C(4) | 2.544(3) | 2.539(2) | Zr−C(7) | 2.264(4) | 2.267(2) |
| Zr−C(5) | 2.561(4) | 2.528(2) | Zr−C(8) | 2.270(3) | 2.255(2) |
| Zr−C(11) | 3.507(4) | 3.416(2) | Zr−C(18) | 2.383(4) | 2.334(2) |
| Zr−C(12) | 4.185(4) | 4.093(2) | Zr−C(17) | 2.520(4) | 2.487(2) |
| Zr−C(13) | 4.171(4) | 4.113(2) | Zr−C(16) | 2.518(4) | 2.501(2) |
| Zr−C(14) | 3.465(4) | 3.452(2) | Zr−C(15) | 2.380(4) | 2.386(2) |
| C(11)−C(12) | 1.350(6) | 1.369(2) | C(18)−C(17) | 1.402(6) | 1.426(3) |
| C(12)−C(13) | 1.419(5) | 1.417(4) | C(17)−C(16) | 1.384(6) | 1.395(3) |
| C(13)−C(14) | 1.366(6) | 1.367(3) | C(16)−C(15) | 1.406(6) | 1.418(3) |
| rotational angle[a] | 177.8(4) | 84.6(2) | | | |
| cent−Zr−cent[b] | 60.7(6) | 61.3(4) | | | |
| $\eta^9$ fold angle[c] | 37.1(3) | 37.6(1) | | | |
| buckle | 4.9(2) | 6.3(2) | | | |

[a] Angle formed between the plane defined by Zr, C(2), and the centroid between C(4)−C(5) and the plane defined by Zr, C(7)−C(8) centroid, and C(16)−C(17) centroid. [b] Angle formed between the zirconium and the centroids of the five- and six-membered rings of the $\eta^9$ indenyl ligands. [c] Angle formed between the intersection of the normal to the planes of the centroid of the five- and six-membered rings of the $\eta^9$ ligands.

Crystallographic characterization of both **3** and **5** provides the first structural evidence for $\eta^9$ metal−indenyl bonding.[42b] For the zirconium sandwich complexes, this interaction affords a formally 18-electron, coordinatively saturated metal center. These molecules are conceptually related to the group 4 transition metal pentalene compounds initially described by Jonas and co-workers.[44] Both "mixed-ring" compounds of the form ($\eta^5$-$C_5H_5$)($\eta^8$-$C_8H_6$)MX (M = Ti, Zr, Hf; X = halide), and homoleptic bis-pentalene complexes ($\eta^8$-$C_8H_6$)$_2$M have been isolated. Solution NMR studies on the latter compounds established molecules of $D_{2d}$ molecular symmetry, consistent with $\eta^8$ coordination of both pentalene ligands, giving the appearance of "20-electron" compounds. Computational studies are inconsistent with this bonding picture, demonstrating that only 9 of the 10 ligand $\pi$-orbitals interact with the metal center,

(41) Katz, T. J. *J. Am. Chem. Soc.* **1960**, *82*, 3784.
(42) (a) Katz, T. J.; Rosenberger, M. *J. Am. Chem. Soc.* **1962**, *84*, 865. (b) The $\eta^9$ indenyl interaction was initially predicted computationally by Verios before the determination of the solid state structures of **3** and **5**. Verios, L. F., manuscript in preparation.
(43) (a) Fessenbecker, A.; Stephan, M.; Grimes, R. N.; Pritzkow, H.; Zenneck, U.; Siebert, W. *J. Am. Chem. Soc.* **1991**, *113*, 3061. (b) Treichel, P. M.; Johnson, J. W. *J. Organomet. Chem.* **1975**, *88*, 207. (c) Bonifaci, C.; Ceccon, A.; Gambaro, A.; Manoli, F.; Mantovani, L.; Ganis, P.; Santi, S.; Venzo, A. *J. Organomet. Chem.* **1998**, *577*, 97. (d) Ceccon, A.; Gambaro, A.; Santi, S.; Valle, G.; Venzo, A. *Chem. Commun.* **1989**, 51.
(44) Jonas, K.; Korb, P.; Kollbach, G.; Gabor, B.; Mynott, R.; Angermund, K.; Heineman, O.; Krüger, C. *Angew. Chem., Int. Ed. Engl.* **1997**, *36*, 1714.

suggesting a more traditional 18-electron molecule.[45] This computational model has also been corroborated by photoelectron spectroscopy.[46]

While the two ligand types are isoelectronic, the resulting bis-indenyl zirconium sandwich complexes have several notable differences from the homoleptic bis-pentalene compounds. Most significantly, dissociation of the neutral benzo portion of the $\eta^9$ ligand would provide a formally 14-electron, $\eta^5,\eta^5$-"zirconocene"-like sandwich and potentially the rich chemistry of such species.[2a,33] In the ground state, the bis-indenyl zirconium sandwiches can be formulated as either Zr(II) compounds, where the coordinated benzo ring functions as a neutral four-electron donor, or Zr(IV) species with an $LX_2$ olefin−alkyl fragment. This redox ambiguity is similar to the bonding scheme encountered with bent zirconocene diene complexes[47] and titanium arene compounds.[48] The metrical parameters of both **3** and **5** (Table 1) establish the importance of the Zr(IV) canonical form (**B**), as the C═C bonds of the coordinated benzo ring are slightly elongated with respect to the corresponding $\eta^5$ ligand. The slight buckling of the coordinated six-membered ring also supports the $LX_2$ bonding description, where the $\sigma$-interactions occur from the C15 and C18 atoms. Coordination of the cyclopentadienyl portion of the indenyl ligand in **3** and **5** attenuates the unsaturation of the zirconium and lessens the importance of the Zr(IV) canonical structures.

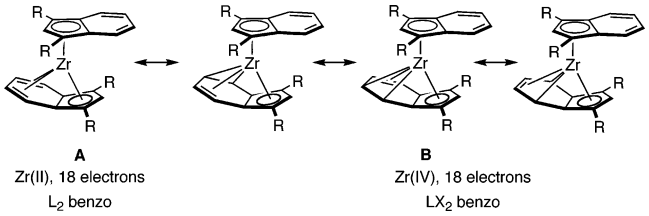


The electronic structure of the zirconium sandwich complexes has been studied in more detail with the aid of density functional theory calculations as implemented by the ADF suite of programs.[49−51] Full molecule geometry optimization of **5** provided a structure in excellent agreement with the experimentally determined structure.[52] A similar computation was conducted on the full molecule of **1**, and the optimized geometry is in good agreement with the solid-state structure of **3**. The HOMO and LUMO of **1** and **5** are similar, and selected orbitals

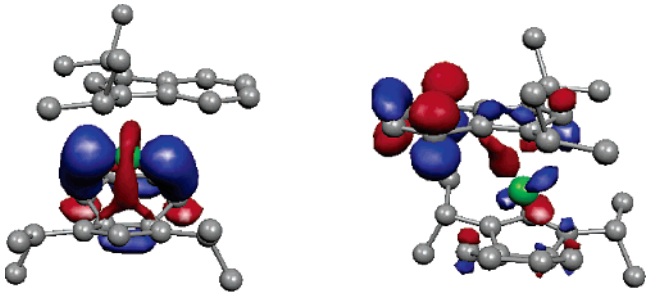


***Figure 5.*** Representations of the HOMO and LUMO of **5** as calculated using ADF (2003.01, TZ2P, ZORA).

for **5** are presented in Figure 5 as representative examples. More detailed frontier molecular orbital diagrams for both molecules are contained in the Supporting Information. The HOMO of **5** (Figure 5) is principally composed of a zirconium $1a_1$ orbital[53] interacting with a linear combination of p-orbitals of the six carbons on the benzo portion of the $\eta^9$ ligand. The major lobe of the zirconium orbital bonds with the p-orbitals on the benzo carbons proximal to the cyclopentadienyl ring. This interaction is augmented by the favorable overlap of the toroid with the p-orbitals of bridgehead carbons as well as those from the benzo carbons distal from the five-membered ring. The LUMO (−1.679 eV) lies 35 kcal/mol above the HOMO and is principally $\pi$-orbitals on the benzo portion of the $\eta^5$ indene that are not engaged in bonding with the zirconium. The large HOMO−LUMO gap is consistent with the observation of a closed shell, coordinatively saturated molecule.

Additional zirconium−ring interactions are observed in the HOMO-1 (−4.747 eV), which principally contains an interaction between a cloverleaf zirconium d-orbital and one of the cyclopentadienyl carbons substituted with an isopropyl group. A similar zirconium−ring interaction is observed in the HOMO-2 (−4.970 eV) orbital that is augmented by additional bonding to the $\eta^5$ indenyl ring. These interactions, in conjunction with HOMO-4 (−6.208 eV), account for the bonding of all nine indenyl carbons with the zirconium. Graphical representations[67] of these orbitals can be found in the Supporting Information.

**NMR Characterization and Solution Dynamics of Homoleptic Bis-indenyl Zirconium Sandwich Complexes.** The solution structure and dynamics of the homoleptic bis-indenyl zirconium sandwich complexes, **1**−**5**, were studied by $^1$H and $^{13}$C NMR spectroscopy in conjunction with two-dimensional *g*-COSY, *g*-HSQC, and *g*-HMBC experiments. Complete assignments for each of the zirconium sandwich complexes are provided in the Experimental Section and Supporting Information. As a representative example, both $^1$H and $^{13}$C spectra of **3** are presented in Figure 6. As previously reported for **1**,[34] both

(45) Costuas, K.; Saillard, J.-Y. *Chem. Commun.* **1998**, 2047.
(46) Gleiter, R.; Bethke, S.; Okubo J.; Jonas, M. *Organometallics* **2001**, *20*, 4274.
(47) Erker, G.; Kruger, C.; Muller, G. *Adv. Organomet. Chem.* **1985**, *24*, 1.
(48) Ozerov, O. V.; Ladipo, F. T.; Patrick, B. O. *J. Am. Chem. Soc.* **1999**, *121*, 7941.
(49) te Velde, G.; Bickelahaupt, F. M.; van Gisbergen, S. J. A.; Fonseca Guerra, C.; Barends, E. J.; Snijders, J. G.; Zielger, T. *J. Comput. Chem.* **2001**, *22*, 931.
(50) Guerra, C. F.; Snijders, J. G.; te Velde, G.; Baerend E. J. *Theor. Chem. Acc.* **1998**, *99*, 391.
(51) Baerends, E. J.; Autschbach, J. A.; Berces, A.; Bo, C.; Boerrigter, P. M.; Cavallo, L.; Chong, D. P.; Deng, L.; Dickson, R. M.; Ellis, D. E.; Fan, L.; Fischer, T. H.; Guerra, C. F.; van Gisbergen, S. J.; Groeneveld, J. A.; Gritsenko, O. V.; Grüning, M.; Harris, F. E.; van den Hoek, P.; Jacobsen, H.; van Kessel, G.; Koostra, F.; van Lenthe, E.; Osinga, V. P.; Patchkovshii, S.; Philipsen, P. H.; Post, D.; Pye, C. C.; Ravenek, W.; Ros, P.; Schipper, P. R.; Schreckenbach, G.; Snijders, J. G.; Sola, M.; Swart, M.; Swerhone, D.; te Velde, G.; Vernooijs, P.; Versluis, L.; Visser, O.; van Wezenbeek, E.; Wiesenekker, G.; Wolff, S.; Woo, T.; Ziegler, T. *ADF 2002.03 SCM Theoretical Chemistry*; Vrije Universiteit: Amsterdam, The Netherlands, http://www.scm.com/.
(52) A calculation on staggered **5** was also performed and provided results similar to those for gauche **5**.
(53) Lauher, J. W.; Hoffmann, R. *J. Am. Chem. Soc.* **1976**, *98*, 1729.
(54) Marat, K. *Spinworks*; University of Manitoba: Manitoba, Canada, 2004.
(55) For a recent example, see: Jahr, H. C.; Nieger, M.; Dötz, K. H. *Chem. Commun.* **2003**, 2866.
(56) (a) Negishi, E.; Kondakov, D. Y. *Chem. Soc. Rev.* **1996**, *26*, 417. (b) Negishi, E.; Takahashi, T. *Bull. Chem. Soc. Jpn.* **1998**, *71*, 755.
(57) Fujita, K.; Shinokubo, H.; Oshima, K. *Angew. Chem., Int. Ed.* **2003**, *42*, 2550.
(58) Fujita, K.; Yorimitsu, H.; Shinokubo, H.; Oshima, K. *J. Am. Chem. Soc.* **2004**, *126*, 6776.
(59) McDade, C.; Bercaw, J. E. *J. Organomet. Chem.* **1985**, *279*, 281.
(60) Swanson, D. R.; Rousset, C. J.; Negishi, E. *J. Org. Chem.* **1989**, *54*, 3521.
(61) Pangborn, A. B.; Giardello, M. A.; Grubbs, R. H.; Rosen, R. K.; Timmers, F. J. *Organometallics* **1996**, *15*, 1518.
(62) Gómez, J. C. C.; López, F. J. S. *MestRe-C*, version 3.7.1.9.0; Universidade de Santiago de Compostela: 2004; www.mestrec.com.

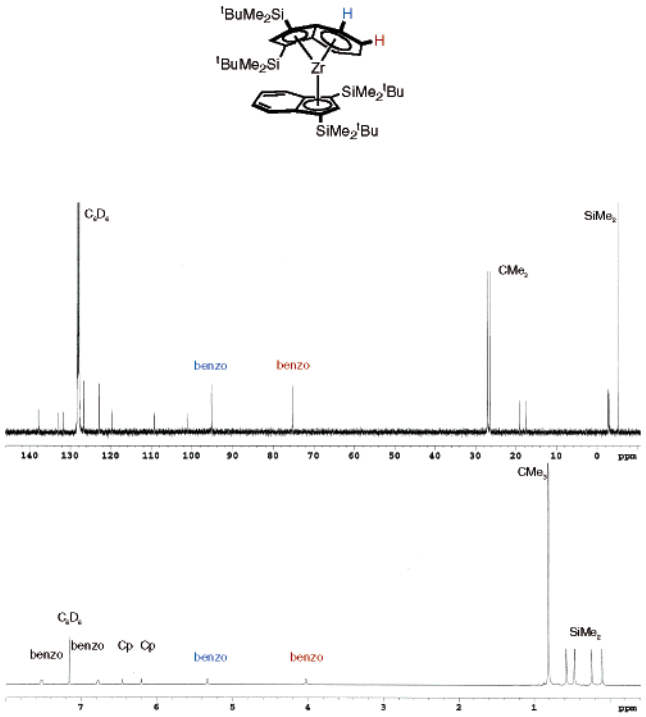


***Figure 6.*** $^{1}$H and $^{13}$C NMR spectrum of **3** in benzene-$d_6$ at 23 °C.

spectra exhibit the number of peaks consistent with a molecule of $C_s$ symmetry with inequivalent indenyl rings. One of the most notable features of the $^{1}$H NMR spectrum of **3** is the resonances centered at 4.02 and 5.37 ppm. Both *g*-COSY and *g*-HMBC experiments establish diagnostic couplings that identify these peaks as benzo resonances on the $\eta^9$ indenyl ring. Similar features are observed in the $^{13}$C spectrum, where upfield-shifted carbons appear at 75.32 and 95.32 ppm for the carbons in the six-membered ring coordinated to the zirconium. In contrast, $\eta^9$ hapticity has little effect on the chemical shift of the cyclopentadienyl hydrogen, as $^{1}$H NMR signals centered at 6.20 and 6.45 ppm are observed for the protons on the inequivalent cyclopentadienyl rings.

The other homoleptic bis-indenyl zirconium sandwich complexes display similar spectral features. However, sandwiches **1**−**5** are dynamic in solution, and cooling the sample below ambient temperature is often required for observation of a static molecule. Variable-temperature $^{1}$H NMR spectroscopy was used to interrogate the dynamics of each zirconium sandwich in toluene-$d_8$ solution. As a representative example, a stack plot of the spectra of **2** as a function of temperature is presented in the Supporting Information. At temperatures below −40 °C, a $C_s$-symmetric molecule is observed with distinct resonances for the benzo and cyclopentadienyl hydrogens. In the static limit, the benzo hydrogens of the $\eta^9$-indenyl ring appear at diagnostic values of 3.66 and 5.56 ppm. Diastereotopic silyl methyl groups are also observed at this temperature. Warming the sample to 2 °C broadens both the benzo and cyclopentadienyl hydrogens and results in coalescence of one set of silyl methyls. At 23 °C, the benzo and cyclopentadienyl hydrogens are nearly broadened into the baseline and both sets of diastereotopic methyl groups appear as singlets.

Similar variable-temperature behavior was observed for the other zirconium sandwich complexes. In all cases, the changes are reversible as repeated warming and cooling cycles regenerate

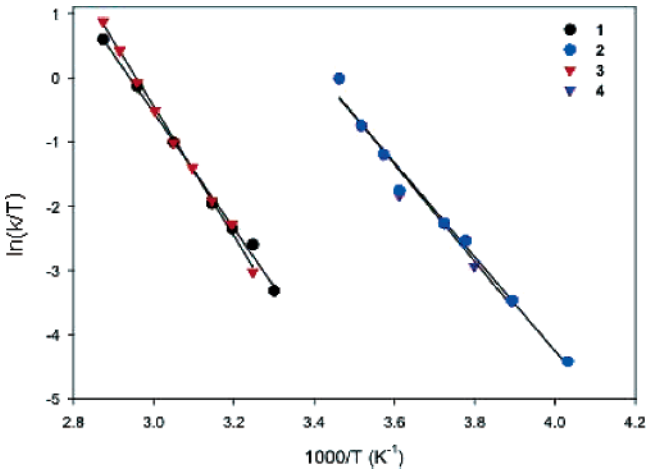


***Figure 7.*** Eyring plots for indenyl ring interconversion for **1**−**4**.

the original spectra. Special care should be exercised in heating **1** as prolonged thermolysis induces approximately 40% conversion to another unidentified compound that most likely derives from cyclometalation of the [$SiMe_3$] substituents. The observed temperature-dependent NMR spectra are consistent with a fluxional process involving interconversion of the $\eta^9$ and $\eta^5$ indenyl ligands on the NMR time scale (eq 4). Notably, the $^{1}$H NMR spectrum of **5** exhibits the number of resonances for a $C_s$-symmetric molecule inconsistent with the solid-state structure which is $C_1$-symmetric, suggesting that ring rotation occurs even when the ring interconversion is frozen out.

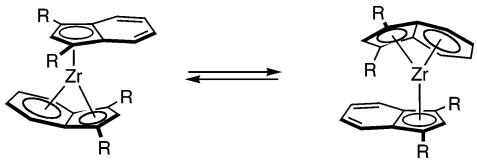


(4)

Rate constants for the ring interchange were measured by a combination of line-shape analysis[54,62] and EXSY NMR experiments.[63] The most reliable line-broadening rate constants were obtained from modeling the silyl and [$CMe_3$] indenyl substituents rather than the cyclopentadienyl or benzo hydrogens. For both **2** and **3**, the observation of two sets of diastereotopic methyl groups provided redundant rate constants that are in good agreement. One exception is **5**, where the peak overlap in the low-temperature spectra prevents an accurate determination of $\Delta\nu_\infty$. For consistency, the rate constants for ring exchange of several other sandwiches were also measured by EXSY and found to be in excellent agreement with the values obtained from line broadening. For example, the rate of ring interconversion for **1** determined by line broadening was 5(1) $s^{-1}$ whereas a value of 6(2) $s^{-1}$ was measured by EXSY.

Ring-exchange rate constants for sandwiches **1**−**4** were determined over a modest range of temperatures, typically between 35 and 50 °C, allowing construction of Eyring plots (Figure 7) and determination of activation parameters (Table 2). For comparison, the relative rates of ring interchange at a common temperature, 23 °C, are also included in Table 2. The values of $\Delta S^{\ddagger}$ range between 2 and 12 eu and are consistent

(63) (a) Perrin, C. L.; Dwyer, T. J. *Chem. Rev.* **1990**, *90*, 935. (b) Derose, E. F.; Castillo, J.; Saulys, D.; Morrison, J. *J. Magn. Reson.* **1991**, *93*, 347. (c) Zolnai, Z.; Juranic, N.; Vikic-Topic, D.; Macura, S. *J. Chem. Inf. Comput. Sci.* **2000**, *40*, 611.

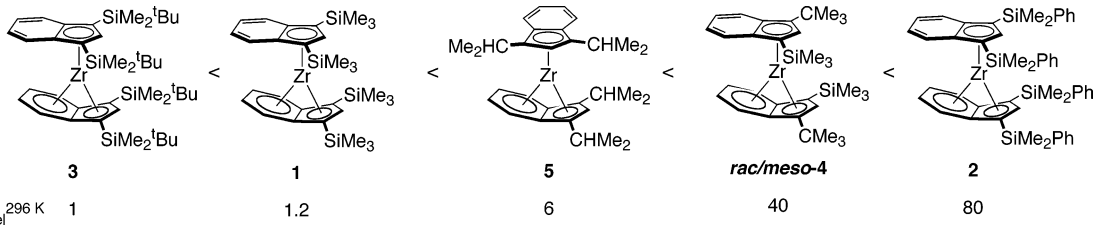


***Figure 8.*** Relative rates of ring interconversion for bis-indenyl zirconium compounds.

***Table 2.*** Activation Parameters and Relative Rates of Ring Interconversion for Homoleptic Bis-indenyl Zirconium Sandwich Complexes

| compound | $\Delta H$ (kcal/mol) | $\Delta S$ (eu) | $\Delta G$ (kcal/mol)[a] | relative rate[a] |
|---|---|---|---|---|
| 1 | 17.9(1) | 6(1) | 16.3(1) | 1.2 |
| 2 | 14.5(3) | 2(1) | 13.8(3) | 80 |
| 3 | 20.4(3) | 12(5) | 16.9(3) | 1 |
| 4 | 15.1(3) | 2(1) | 14.4(3) | 40 |
| 5 | NA[b] | NA | 19.9(5)[c] | 6 |

[a] $T = 296$ K. [b] Not determined due to overlapping resonances. [c] Determined from a single rate constant at 296 K.

with a unimolecular, dissociative process. From these results the relative rates of $\eta^5 \rightarrow \eta^9$ ring interconversion have been measured as a function of indenyl substituent (Figure 8). A discussion of the rates and possible mechanisms for ring interconversion will be presented in a later section.

**Synthesis of Heteroleptic Bis-indenyl Zirconium Sandwich Complexes.** Introduction of two chemically distinct indenyl ligands into the coordination sphere of the zirconium raises the question of what (if any) preference would be observed for $\eta^9$ coordination. To test this hypothesis, the synthesis of several heteroleptic bis-indenyl zirconium complexes was explored. Treatment of **6-Cl$_2$** with two equivalents of $LiCH_2CHMe_2$ rapidly produced isobutene from hydride transfer and isobutane from reductive elimination, along with the desired sandwich complex, **6** (eq 5). The $^1$H NMR spectrum of **6** in benzene-$d_6$

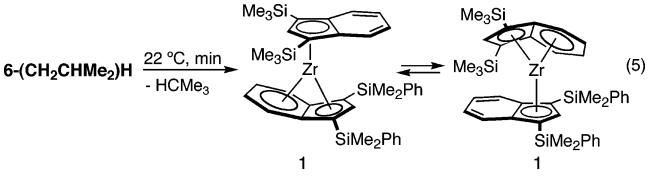


exhibits twice the number of resonances in equal ratios expected from a single $C_s$-symmetric bis-indenyl zirconium sandwich. Similar behavior is observed by $^{13}$C NMR spectroscopy. Subsequent EXSY NMR experiments on the mixture of compounds demonstrate facile exchange between the two isomers (eq 5). Thus, for this sandwich there is no measurable preference for either ring to adopt $\eta^9$ coordination.

Similar synthetic procedures were used to prepare the other heteroleptic sandwiches, **7**, **8**, and **9** (Figure 2). In all three cases, only one isomer was detected by $^1$H and $^{13}$C NMR spectroscopy. A series of two-dimensional NMR experiments were conducted to assign the identity of each observed isomer and determine the preference for $\eta^9$ coordination. Establishment of connectivity and differentiation between cyclopentadienyl and benzo peaks was accomplished by a combination of *g*-COSY, *g*-HMBC, and *g*-HSQC experiments. As a representative example, the benzo and cyclopentadienyl region of the *g*-COSY spectrum of **7** is shown in Figure 9. The two resonances centered at 6.09 and 6.40 ppm do not couple to any other peaks, identifying them as cyclopentadienyl hydrogens. The remaining four upfield resonances are therefore assigned as the four inequivalent hydrogens on the benzo portion of the $\eta^9$-indenyl ring. Through-bond coupling was established by a *g*-COSY experiment and identified the resonances at 5.17 and 5.45 ppm as the benzo hydrogens proximal to the five-membered ring, whereas those centered at 3.82 and 4.07 ppm are distal. Similar analyses were used to establish connectivity in **8** and **9**. Spectral assignments for all three molecules can be found in the Experimental Section and Supporting Information.

While through-bond coupling experiments established connectivity, these data do not identify which ligand is engaged in the $\eta^9$ interaction. A series of NOESY experiments were conducted on **7**, **8**, and **9** to determine the identity of the preferred isomer. As a representative example, the assignment of **9** will be presented in detail. Cross-peaks in the −40 °C NOESY spectrum were observed between the [$CMe_3$] resonance (1.37 ppm) and one cyclopentadienyl (5.02 ppm), one isopropyl methine (3.34 ppm), and three benzo hydrogens. Importantly, one of the benzo resonances (7.68 ppm) is in the $\eta^5$ indenyl region, while the two others (4.04 and 5.37 ppm) are in the

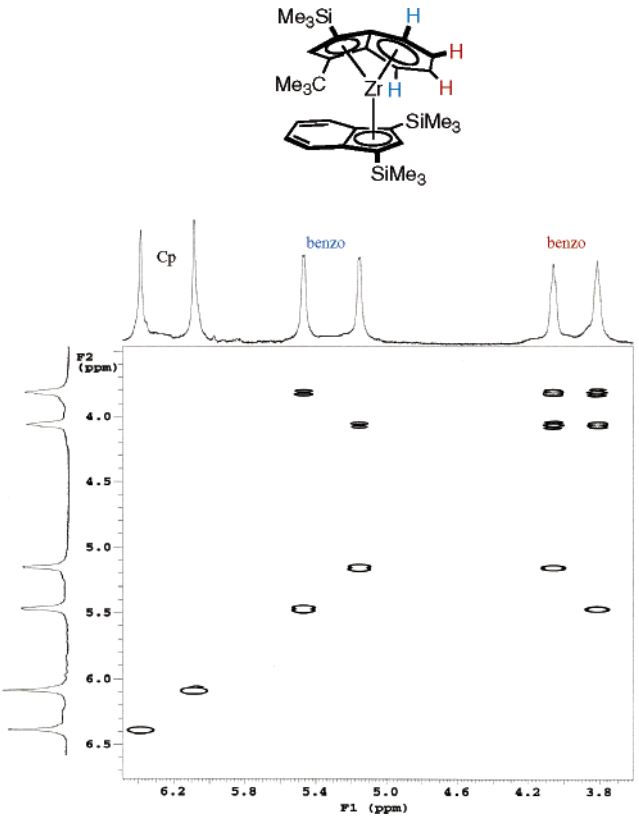


***Figure 9.*** Indenyl region of the *g*-COSY NMR spectrum of **7** in benzene-$d_6$ at 21 °C.

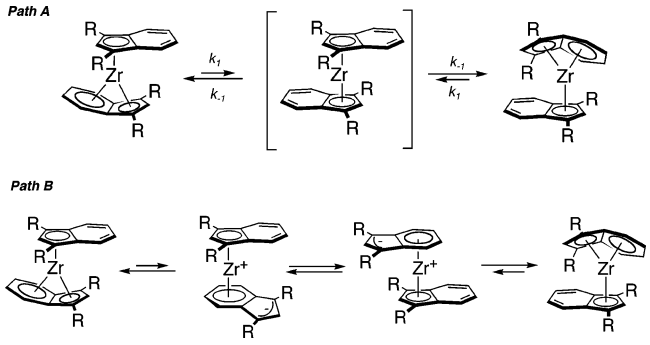


***Figure 10.*** Possible pathways for $\eta^5 \rightarrow \eta^9$-indenyl interconversion of bis-indenyl zirconium sandwich complexes.

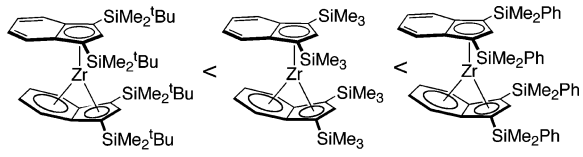


| | **3** | **1** | **2** |
|---|---|---|---|
| $k_{rel}^{296\ K}$ | 1 | 1.2 | 80 |
| ν(CO): | 1976, 1895 | 1980, 1901 | 1982, 1902 |
| E° (mV): | -122 | -118 | -20 |

***Figure 11.*** Relative rate of ring interconversion, carbonyl stretching frequencies of the corresponding zirconocene dicarbonyl, and oxidation potential of the bis-indenyl iron sandwiches.

diagnostic $\eta^9$ portion of the spectrum. Because no cross-peak was observed between the [$CMe_3$] group and any distal hydrogen on the $\eta^5$ indenyl, this substituent must be on the $\eta^5$ ring. Enhancements in the other two benzo hydrogens are a result of transannular NOE effects on the $\eta^9$ ligand. Complimentary cross-peaks to the other benzo resonances were observed with the [$SiMe_3$] substituent. Similar cross-peaks involving the [$CHMe_2$] groups as well as other benzo resonances were observed and allowed complete assignment of the $^1$H NMR spectrum.

Performing the NOESY at 22 °C produced similar cross-peaks, although the $\eta^9-\eta^5$ through-space interactions were reduced. Significantly, weak but observable exchange peaks are also observed with a minor isomer present in ~1% of the mixture. These data clearly establish the thermodynamic preference for the $\eta^9$ coordination of the isopropyl-substituted ligand, although the minor isomer is kinetically accessible. Similar data were collected on **7** and **8** and allowed assignment of the major isomer in both cases. In all three heteroleptic sandwich complexes, the more alkylated indenyl ring preferentially adopts $\eta^9$ coordination (Figure 2).

Observation of a single isomer of **7** as compared to the near equimolar mixture observed for **6** highlights the influence of indenyl substitution on the ground-state preferences for $\eta^9$ coordination. Replacement of a single silyl group with an alkyl substituent perturbs the equilibrium such that predominantly one isomer is observed in solution. The synthesis of single isomers of **8** and **9** also corroborates the finding that alkylated indenyl ligands prefer $\eta^9$ hapticity. Previous studies from our laboratory have established that alkylated indenyl ligands are more electron donating than their silylated counterparts.[35] Preferential interaction of the more electron-donating benzo ring suggests that $\pi$-donation from the coordinated six-membered ring is a key component of metal$-\eta^9$ indenyl bonding, supporting a significant contribution from the zirconium(II) diolefin adduct.

**Possible Mechanisms for Ring Interchange.** Both the homo- and heteroleptic bis-indenyl zirconium sandwich complexes are dynamic in solution. Examining the frontier molecular orbitals of the sandwiches (Figure 5 and Supporting Information) suggests that dissociation of the benzo portion of the $\eta^9$ indenyl ligand to afford a symmetric $\eta^5,\eta^5$ intermediate appears to be a plausible pathway for ring interconversion (Figure 10, Path A). Experimental support for this pathway is provided by the reaction of **1** with CO, alkynes, and (dimethylamino)pyridine to afford bent zirconocene complexes with familiar $\eta^5,\eta^5$ coordination of the indenyl ligands.[34] Although a detailed kinetic study has not been performed, it is likely that ligand addition to the 18-electron, coordinatively saturated zirconium sandwich proceeds via initial dissociation of the benzo ring to afford a reactive $\eta^5,\eta^5$ zirconium sandwich intermediate.

Alternatively, a mechanism involving formally zwitterionic $\eta^5,\eta^6$ sandwich intermediates can also be envisioned (Figure 10, Path B). Isolation and crystallographic characterization of an $\eta^5,\eta^6$ zirconocene−THF complex[34] suggests that dissociation of the five-membered ring is viable. It is important to note, however, that in this mechanism the $\eta^6$ indenyl ligand must undergo a haptotropic rearrangement in order to interconvert the two rings. Computational studies by Albright et al.[39] demonstrated the feasibility of such ring migrations, and several such rearrangements have been observed experimentally, most frequently in group 6 arene chemistry.[55] The computational studies also suggest that ring migration through $\eta^3$-allylic intermediates are energetically favorable as rearrangement through the center of the polycyclic rings is symmetry forbidden.[39] A concerted pathway that interchanges the two indenyl rings also cannot be excluded.

Attempts to distinguish between these pathways experimentally have not been successful. While modest substituent effects have been observed for the rate of ring interconversion, no obvious trend has emerged that favors one pathway. The rate of fluxionality versus electronic parameters for purely silyl-substituted zirconium sandwiches is presented in Figure 11. Both carbonyl stretching frequencies on the corresponding zirconocene dicarbonyl compounds and electrochemistry on related bis-indenyl iron sandwiches[35] have established the relative electrophilicity of each zirconocene as **3** < **1** < **2**. The ordering of the electronic properties of the silylated zirconium sandwiches correlates with their electronic parameters, although the effects are quite small. Our previous studies demonstrated that the electronic properties of **1** and **3** are almost indistinguishable as are the rates of ring interconversion.[35] In contrast, **2** is much more electrophilic, and as a consequence, the rate of the fluxional process increases dramatically as compared to **1** and **3**. It is interesting to note that the two most sterically hindered complexes are at opposite ends of the series.

A possible explanation for this trend could be ground-state destabilization of benzo ring coordination based on observations that the most electron-donating indenyl ligand adopts $\eta^9$ coordination. However, the relative rates of ring interconversion for the alkylated zirconium sandwiches, **4** and **5**, do not support this reasoning. Taken as a whole, the relative rates of indenyl ring interchange are slightly dependent on the substituents and a composite of both ground- and transition-state effects that are not readily delineated based on the data collected.

**Reaction of Bis-indenyl Zirconium Sandwiches with Unsaturated Organic Molecules.** Synthesis and characterization of bis-indenyl zirconium sandwich complexes prompted an exploration of their utility in traditional "zirconocene"-promoted reactions with olefins and alkynes.[3a] Because a series of isolable zirconium sandwiches has been prepared, there is a unique opportunity to tune the stereoelectronic properties of the reagent, perhaps for specifically tailored applications. As noted in a previous section, preparation of the alkylated zirconium sandwich **5** by treatment of **5-Cl$_2$** with two equivalents of isobutyllithium produced the bis-indenyl zirconium methyl allyl hydride complex **5-($\eta^3$-CH$_2$C(Me)CH$_2$)H** (eq 6). Isolation of

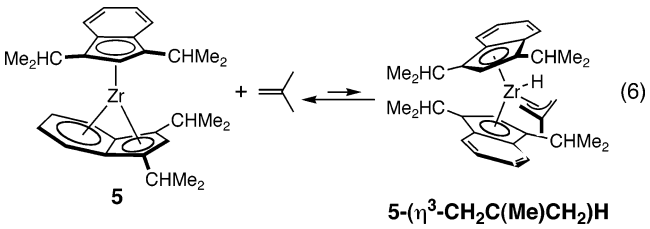


(6)

yellow **5-($\eta^3$-CH$_2$C(Me)CH$_2$)H** using this method is best achieved in a closed system so that the isobutene cannot escape. This C−H activation side reaction was not observed during the synthesis of any other zirconium sandwich, highlighting the increased propensity of **5** to participate in formal oxidative addition reactions. The origin of this effect is 2-fold. The presence of alkylated indenyl ligands produces a relatively electron-rich zirconium that favors C−H bond addition.[35] Moreover, this sandwich is the most open member of the series, thus favoring the approach and activation of the olefin.

Synthesis of **5-($\eta^3$-CH$_2$C(Me)CH$_2$)H** has also been independently accomplished by addition of excess isobutene to the sandwich. Working with isolated compound revealed that the C−H activation reaction is reversible; reductive elimination of isobutene is observed in solution over the course of hours at ambient temperature. Characterization of **5-($\eta^3$-CH$_2$C(Me)CH$_2$)H** has been accomplished by NMR spectroscopy, elemental analysis, and X-ray diffraction. The solid-state structure of the molecule is presented in Figure 12. As we observed previously,[34] oxidative addition of a C−H bond to the zirconium sandwich restores the more commonly observed $\eta^5,\eta^5$ hapticity of the indenyl ligands. In contrast to the gauche conformation observed in the solid-state structure of **5**, the ring orientation in **5-($\eta^3$-CH$_2$C(Me)CH$_2$)H** is staggered with a rotational angle of 179.4(3)°. This change in conformation most likely arises from a gearing effect induced by the methyl group on the allyl ligand. To maximize bonding to the $\pi$-allyl, the methyl group must point directly toward one of the indenyl ligands. As a result, the ring orients such that the methyl substituent is nestled between the two isopropyl groups whose methine hydrogens are directed toward the interior of the metallocene. The other ring then staggers with respect to the first to minimize transannular interactions.

Characterization of **5-($\eta^3$-CH$_2$C(Me)CH$_2$)H** by solution $^1$H and $^{13}$C NMR spectroscopy revealed a dynamic molecule at ambient temperature. Variable-temperature NMR studies are consistent with $\eta^1,\eta^3$ allyl interconversion as well as hydride transfer between the zirconium and the allyl fragments.[58] The full details of these experiments will be published elsewhere. Identification of both $^1$H and $^{13}$C resonances has been achieved

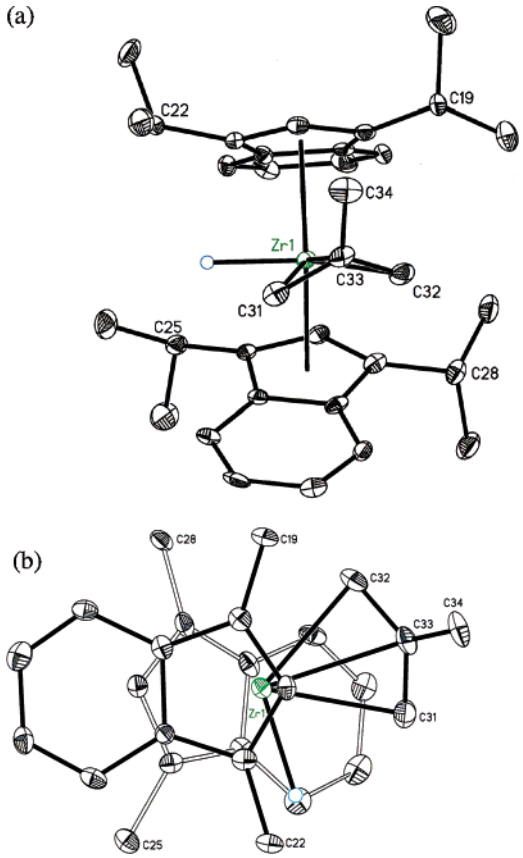


***Figure 12.*** (a) Molecular structure of **5-($\eta^3$-CH$_2$C(Me)CH$_2$)H** at 30% probability ellipsoids. Hydrogen atoms, except the zirconium hydride, omitted for clarity. (b) Top view of the molecule with isopropyl substituents and hydrogen atoms, except for the zirconium hydride, omitted for clarity.

***Table 3.*** Selected Bond Distances for **5-($\eta^3$-CH$_2$C(Me)CH$_2$)H**

| | bond distance (Å) |
|---|---|
| Zr(1)−C(31) | 2.486(6) |
| Zr(1)−C(32) | 2.407(5) |
| Zr(1)−C(33) | 2.571(5) |
| C(31)−C(33) | 1.366(8) |
| C(32)−C(33) | 1.409(7) |
| C(33)−C(34) | 1.517(7) |

at temperatures below −38 °C, where the molecule is in the static limit. In this regime, the spectra exhibit the number of resonances expected for a $C_1$-symmetric molecule. Assignment of each hydrogen and carbon was accomplished through a combination of *g*-COSY, *g*-HSQC, and *g*-HMBC experiments and is reported in detail in the Experimental Section.

Given the importance of the transient zirconocene 1-butene complex, ($\eta^5$-C$_5$H$_5$)$_2$Zr($\eta^2$-CH$_2$═CHCH$_2$CH$_3$), in Negishi-type coupling reactions,[56] we explored the reactivity of the bis-indenyl zirconium sandwiches with α-olefins. Careful addition of one equivalent of 1-butene to **5** affords a yellow compound identified as **5-($\eta^3$-CH$_2$CHC(Me)H)H** on the basis of multinuclear NMR experiments (eq 7). This molecule can also be prepared by addition of either *cis*- or *trans*-2-butene to the sandwich. As expected, the internal alkenes react much slower than the terminal olefin.

As with **5-($\eta^3$-CH$_2$C(Me)CH$_2$)H**, **5-($\eta^3$-CH$_2$CHC(Me)H)-H** is dynamic in solution, requiring temperatures below −40 °C for observation of spectra in the static limit. A combination of low-temperature *g*-HSQC and *g*-HMBC experiments was

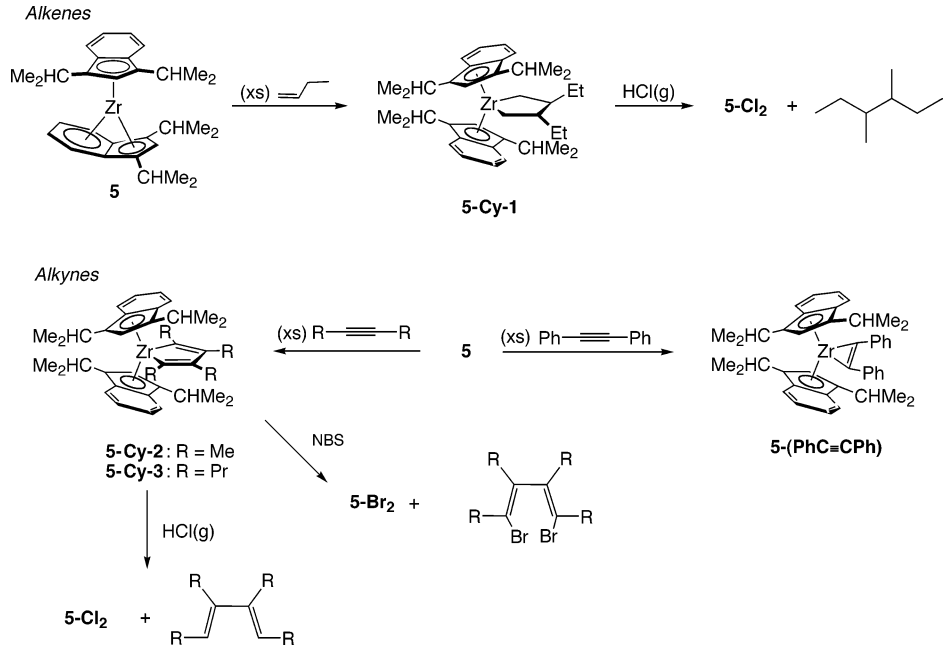


***Figure 13.*** Reactivity of **5** with olefins and alkynes.

used to assign the allylic carbons, while *g*-COSY data allowed differentiation and assignment of the benzo, cyclopentadienyl, and zirconium−hydride resonances. Importantly, **5-($\eta^3$-$CH_2CHC$(Me)H)H** is more resistant to reductive elimination of olefin than **5-($\eta^3$-$CH_2C$(Me)$CH_2$)H**, consistent with observations in cyclopentadienyl chemistry where more substituted zirconocene alkyl hydride complexes participate in more facile reductive elimination processes.[38]


Isolation of **5-($\eta^3$-$CH_2CHC$(Me)H)H** contrasts the behavior and stability of the parent zirconocene-1-butene complex. Dioumaev and Harrod[19] demonstrated that $(\eta^5\text{-}C_5H_5)_2Zr(\eta^2\text{-}CH_2{=}CHCH_2CH_3)$ is in equilibrium with the zirconocene allyl hydride, although the equilibrium favors the olefin complex. Recently, Oshima and co-workers were able to exploit this dynamic phenomenon by performing tandem reductions of 1,4-diketones by delivering both a hydride and an allylic fragment from the zirconium.[57,58] In **5-($\eta^3$-$CH_2CHC$(Me)H)H** the increased electron density imparted by the alkylated indenyl ligands favors oxidative addition of the allylic C−H bond. Similar preferences have been observed in permethylzirconocene chemistry where several allyl hydride complexes have been isolated.[59] Unfortunately attempts to prepare similar compounds with zirconocenes with electron-withdrawing indenyls such as **1** and **2** have yielded a complex mixture of products.

Despite observation of allylic activation in the ground state, both **5** and **5-($\eta^3$-$CH_2CHC$(Me)H)H** participate in coupling reactions that involve the intermediacy of the $\eta^2$-olefin compound. Addition of an excess of 1-butene to either **5** or **5-($\eta^3$-$CH_2CHC$(Me)H)H** resulted in selective coupling of the alkenes to afford the zirconacyclopentane, **5-Cy-1** (Figure 13). As observed in cyclopentadienyl chemistry,[60] the alkyl groups are positioned at the $\beta$ and $\beta'$ positions on the ring. In addition, both the $^1$H and $^{13}$C NMR spectra of **5-Cy-1** are consistent with a molecule of $C_2$ symmetry, establishing the trans disposition of the two ethyl substituents. Treatment of **5-Cy-1** with gaseous hydrogen chloride afforded the zirconocene dichloride complex **5-$Cl_2$** and 3,4-dimethylhexane. Identification of the alkane was accomplished by comparison of NMR and mass spectral data to an authentic sample. Reaction of the zirconacyclopentane with *N*-bromosuccinimide (NBS) produced no reaction.

The bis-indenyl zirconium sandwich complexes also promote the coupling of alkynes. Addition of an excess of either 2-butyne or 4-octyne to **5** furnished the corresponding zirconacyclopentadiene in near quantitative yield (Figure 13). Addition of HCl produced **5-$Cl_2$** and the corresponding diene, whereas reaction with NBS afforded **5-$Br_2$** and the dibromoalkene. Attempts to observe the zirconium alkyne adduct by addition of one equivalent of 2-butyne to **5** have been unsuccessful, producing a near equimolar mixture of the zirconacyclopentadiene and the starting sandwich. A stable alkyne adduct can be isolated upon reaction with diphenylacetylene, although no coupling is observed when this adduct is exposed to excess PhC≡CPh or 2-butyne (Figure 13).

Silylated zirconocene sandwiches participate in similar chemistry depending on both the silyl group and alkyne. For **1**, addition of one equivalent of 2-butyne allows observation of the adduct whereas addition of excess alkyne yields the zirconacyclopentadiene (Figure 14). Similar reactivity is observed with **2**, where the alkyne adduct is observed upon stoichiometric addition of alkyne and zirconocyclopentadiene is obtained in the presence of excess 2-butyne. Treatment of the latter compound with NBS afforded the dibromoalkene and **2-$Br_2$** (Figure 14).

The bis-indenyl zirconium sandwich with the largest silyl substituents, **3**, displays unique reactivity that reflects the increased steric bulk of the ligand array. Treatment with an excess of 2-butyne affords the corresponding alkyne adduct

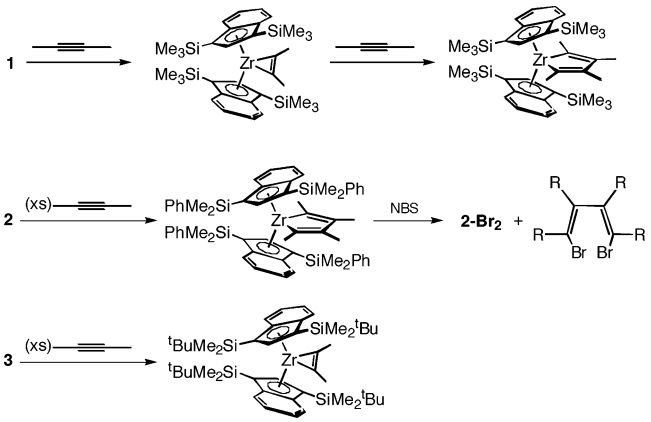


***Figure 14.*** Reactivity of silylated bis-indenyl zirconium sandwich complexes with alkynes.

**3-(MeC≡CMe)**. No additional chemistry is observed upon addition of excess alkyne. Addition of diphenylacetylene to **3** produced no reaction.

## Concluding Remarks

A series of isolable bis-indenyl zirconium sandwich complexes has been prepared by either alkane reductive elimination or reduction with sodium amalgam. Crystallographic characterization of two examples establishes unprecedented $\eta^9$ coordination of one of the indenyl ligands, providing coordinatively saturated molecules and a new binding mode for a ubiquitous organometallic ligand. NMR spectroscopic studies revealed dynamic molecules in solution, where the $\eta^5$ and $\eta^9$ rings are interconverting on the time scale of the NMR experiment. In analogy to "zirconocene" chemistry, the bis-indenyl zirconium sandwiches react with olefins and alkynes to form zirconacycles with restored $\eta^5,\eta^5$ hapticity. Isolation of the intermediate olefin complexes reveals that the equilibrium lies toward the zirconocene allyl hydride arising from C−H activation of an allylic hydrogen. The results of these studies have provided a family of isolable "zirconocene" reagents that can be easily tuned by judicious choice of indenyl substituents.

## Experimental Section

**General Considerations.** All air- and moisture-sensitive manipulations were carried out using standard vacuum line, Schlenk, or cannula techniques or in a M. Braun inert atmosphere drybox containing an atmosphere of purified nitrogen. Solvents for air- and moisture-sensitive manipulations were initially dried and deoxygenated using literature procedures.[61] Benzene-$d_6$ and toluene-$d_8$ for NMR spectroscopy were distilled from sodium metal under an atmosphere of argon and stored over 4 Å molecular sieves or sodium metal. All calibrated gas bulb additions used a 31.6 mL calibrated gas bulb. Preparation of all zirconocene dichloride complexes,[35] **1**,[34] and **1-THF**[34] was accomplished as described previously. Isobutylene and 2-butyne were purchased from Aldrich and dried over molecular sieves before use. Diphenylacetylene was purchased from Acros and dried on the high vacuum line followed by recrystallization from dry pentane at −35 °C. 1-Butene and *cis*- and *trans*-2-butene were purchased from Matheson and stored over $LiAlH_4$ before use.

$^1$H and $^{13}$C NMR spectra were recorded on a Varian Inova 400 Spectrometer operating at 399.779 ($^1$H) and 110.524 MHz ($^{13}$C). All chemical shifts are reported relative to $SiMe_4$ using $^1$H (residual) or $^{13}$C NMR chemical shifts of the solvent as a secondary standard. Variable-temperature and two-dimensional NMR experiments were performed on a Varian Inova 500 Spectrometer operating at 499.920 MHz for $^1$H and 125.704 MHz for $^{13}$C. The temperature for the VT experiments was calibrated using methanol and ethylene glycol standards. Line-shape analyses were performed using DNMR as implemented by Spinworks 2.2.[54]

Qualitative EXSY spectra were acquired with a sweep width of 4.2 kHz and a mixing time of 200 ms in phase-sensitive mode. For quantitative rate studies, mixing times of 200, 50, 20, 10, 5, and 1 ms were used. A total of 200 complex points were collected in the indirectly detected dimension with 16 scans and 2k points per increment. The resulting matrix was zero filled to 1k × 1k complex data points, and Gaussian line-broadening functions were applied in both dimensions prior to Fourier transform. Cross-peak integration was performed in Mest-ReC,[62] intensities were normalized, and rates were calculated using literature methods.[63]

NOESY spectra were acquired with a sweep width of 4.8 kHz and a mixing time of 200 ms in phase-sensitive mode. A total of 200 complex points were collected in the indirectly detected dimension with 16 scans and 2k points per increment. The resulting matrix was zero filled to 1k × 1k complex data points, and Gaussian line-broadening functions were applied in both dimensions prior to Fourier transform. All 2D spectra were acquired at 22 °C unless otherwise noted. Details about more routine two-dimensional experiments can be found in the Supporting Information.

Calculations were performed with the Amsterdam Density Functional Theory (ADF2003.01) suite of programs. Relativistic effects were included using the zero-order regular approximation (ZORA). The Vosko, Wilk, and Nusair (VWM) local density approximation,[64] Becke's exchange,[65] and Perdew's correlation[66] (BP86) were used. The cores of the atoms were frozen up to 1s for C and N and 2p for Zr and Si. Uncontracted Slater-type orbitals (STOs) of triple-$\zeta$ quality with two polarizations were employed. This basis set is denoted TZ2P in the ADF program. Each geometry optimization was carried out without symmetry constraints. Orbital pictures were generated using MOLEKEL[67] to process the ADF results.

Single crystals suitable for X-ray diffraction were coated with polyisobutylene oil in a drybox and quickly transferred to the goniometer head of a Siemens SMART CCD area detector system equipped with a molybdenum X-ray tube ($\lambda$ = 0.710 73 Å). Preliminary data revealed the crystal system. A hemisphere routine was used for data collection and determination of lattice constants. The space group was identified, and the data were processed using the Bruker SAINT program and corrected for absorption using SADABS. The structures were solved using direct methods (SHELXS) completed by subsequent Fourier synthesis and refined by full-matrix least-squares procedures. Elemental analyses were performed at Robertson Microlit Laboratories, Inc., in Madison, NJ. Mass spectrometry was performed on a Hewlett-Packard 5980A GC/MS equipped with a 5970 mass-selective detector and a DB-1, 0.25 $\mu$m film, fused silica capillary column with an injection temperature of 35 °C, a ramp rate of 10 °C, and a final column temperature of 260 °C. The organic products were characterized by comparison to literature reports.[68]

**Observation of ($\eta^5$-$C_9H_5$-1,3-($SiMe_2Ph$)$_2$)$_2$Zr($CH_2CHMe_2$)H (2-($CH_2CHMe_2$)H).** A J. Young NMR tube was charged with 20 mg (0.024 mmol) of **2** and 3 mg (0.047 mmol) of $LiCH_2CHMe_2$. Benzene-$d_6$ was then added by pipet, and the tube was sealed with a Teflon valve. The tube was shaken, and the reaction was monitored by $^1$H NMR spectroscopy over the course of 2 h. $^1$H NMR (benzene-$d_6$): $\delta$ = −1.65 (br s, 1H, C*H*$_2$CH(CH$_3$)$_2$), 0.52 (s, 6H, Si*Me*$_2$Ph), 0.54 (s, 6H, Si*Me*$_2$Ph), 0.67 (s, 6H, Si*Me*$_2$Ph), 0.69 (s, 6H, Si*Me*$_2$Ph), 0.86 (d,

(64) Vosko, S. H.; Wilk, L.; Nusair, M. *Can. J. Phys.* **1990**, *58*, 1200.
(65) Becke, A. D. *Phys. Rev.* **1988**, *A38*, 2398.
(66) Perdew, J. P. *Phys. Rev.* **1986**, *B33*, 8822.
(67) Flukiger, P.; Luthi, H. P.; Portmann, S.; Weber, J. *MOLEKEL 4.3*; Swiss Center for Scientific Computing: Manno, 2000; http://www.cscs.ch/molekel.
(68) Takahashi, T.; Yanzhong, L. *Titanium and Zirconium in Organic Synthesis*; Marek, I., Ed.; Wiley-VCH: Weinheim, 2002; Chapter 2.

8 Hz, 6H, $CH_2CH(CH_3)_2$), 2.38 (br m, 1H, $CH_2CH(CH_3)_2$), 6.23 (s, 1H, Zr-*H*), 6.52 (s, 2H, Cp), 7.08−7.18 (br m, 20H, Ph), 7.23 (m, 2H, Ind), 7.39 (m, 2H, Ind), 7.46 (m, 2H, Ind), 7.62 (m, 2H, Ind). One $CH_2CH(CH_3)_2$ resonance not located.

**Preparation of ($\eta^5$-$C_9H_5$-1,3-($SiMe_2Ph$)$_2$)($\eta^9$-$C_9H_5$-1,3-($SiMe_2Ph$)$_2$)-Zr (2).** A 100 mL round-bottomed flask was charged with 0.800 g (0.86 mmol) of **2-Cl$_2$** and approximately 30 mL of toluene forming a yellow solution. At ambient temperature, 0.121 g (1.89 mmol) of $LiCH_2CHMe_2$ was added and the reaction mixture was stirred for 1 h. The resulting burgundy solution was filtered through a pad of Celite, and the solvent was removed in vacuo, leaving a burgundy oil. Recrystallization from pentane at −35 °C afforded 0.291 g (39%) of **2**. Anal. Calcd for $C_{50}H_{54}Si_4Zr$: C, 69.95; H, 6.34. Found: C, 69.69; H, 5.94. $^1$H NMR (toluene-$d_8$, −34 °C): $\delta$ = 0.39 (s, 6 H, Si$Me_2$Ph), 0.44 (s, 6 H, Si$Me_2$Ph), 0.70 (br s, 6 H, Si$Me_2$Ph), 0.74 (br s, 6 H, Si$Me_2$Ph), 3.66 (br s, 2H, Ind), 5.56 (br s, 2H, Ind), 5.86 (s, 1H, Cp), 5.97 (s, 1H, Cp), 6.62 (m, 2H, Ind) 7.13 (br s, 12H, Ph), 7.36 (br s, 8H, Ph), 7.48 (m, 2H, Ind). $^{13}$C NMR (toluene-$d_8$, −34 °C) $\delta$ = −0.25 (Si$Me_2$Ph), −0.09 (Si$Me_2$Ph), 1.35 (Si$Me_2$Ph), 1.55 (Si$Me_2$Ph), 75.10, 95.02 (Ind), 98.25, 110.30, 123.90, 126.57 (Cp), 128.46, 128.68, 129.61, 131.86, 132.98, 134.51, 134.59, 134.85, 137.62, 138.07, 140.26, 140.44 (Ind/Ph).

**Preparation of ($\eta^5$-$C_9H_5$-1,3-($SiMe_2$$^t$Bu)$_2$)($\eta^9$-$C_9H_5$-1,3-($SiMe_2$$^t$Bu)$_2$)-Zr (3).** This molecule was synthesized using a procedure similar to that described for **2** with 0.545 g (0.64 mmol) of **3-Cl$_2$** and 0.086 g (1.3 mmol) of $LiCH_2CHMe_2$, yielding 0.203 g (40%) of **3** as a burgundy solid. Anal. Calcd for $C_{42}H_{70}Si_4Zr$: C, 64.79; H, 9.06. Found: C, 64.45; H, 8.90. $^1$H NMR (benzene-$d_6$): $\delta$ = 0.10 (s, 6H, Si$Me_2$$^t$Bu), 0.24 (s, 6H, Si$Me_2$$^t$Bu), 0.47 (s, 6H, Si$Me_2$$^t$Bu), 0.58 (s, 6H, Si$Me_2$$^t$Bu), 0.81 (s, 36H, SiMe$_2$$^t$*Bu*), 4.02 (s, 2H, Ind), 5.37 (s, 2H, Ind), 6.20 (s, 1H, Cp), 6.45 (s, 1H, Cp), 6.77 (s, 2H, Ind), 7.52 (s, 2H, Ind). $^{13}$C NMR (benzene-$d_6$): $\delta$ = −5.12 (2 Si$Me_2$$^t$Bu), −3.08 (Si$Me_2$$^t$Bu), −2.76 (Si$Me_2$$^t$Bu), 17.42 (SiMe$_2$*C*Me$_3$), 19.03 (SiMe$_2$*C*Me$_3$), 26.46 (SiMe$_2$C*Me$_3$*), 26.99 (SiMe$_2$C*Me$_3$*), 75.32, 95.32 (Ind), 101.21, 109.23, 119.82, 122.81 (Cp), 126.76, 131.68, 132.87, 137.90 (Ind).

**Preparation of *rac/meso*-($\eta^5$-$C_9H_5$-1-($SiMe_3$)-3-($CMe_3$))($\eta^9$-$C_9H_5$-1-($SiMe_3$)-3-($CMe_3$))Zr (4).** This molecule was prepared in an identical manner to **2** with 0.745 g (1.15 mmol) of ***rac*/*meso*-4-Cl$_2$** and 0.151 g (2.36 mmol) of $LiCH_2CHMe_2$, yielding 0.140 g (21%) of a burgundy solid identified as a near equimolar mixture of ***rac*/*meso*-4**. Anal. Calcd for $C_{32}H_{46}Si_2Zr$: C, 66.48; H, 8.03. Found: C, 65.98; H, 7.98. $^1$H NMR (toluene-$d_8$, -34 °C): $\delta$ = 0.21 (s, 9H, Si$Me_3$), 0.30 (s, 9H, Si$Me_3$), 0.34 (s, 9H, Si$Me_3$), 0.38 (s, 9H, Si$Me_3$), 1.23 (s, 9H, C$Me_3$), 1.29 (s, 9H, C$Me_3$), 1.30 (s, 9H, C$Me_3$), 1.34 (s, 9H, C$Me_3$), 3.71 (t, 5 Hz, 1H, Ind), 3.88 (t, 5 Hz, 1H, Ind), 3.94 (t, 5 Hz, 1H, Ind), 4.21 (t, 5 Hz, 1H, Ind), 5.11 (m, 2H, Ind), 5.37 (d, 5 Hz, 1H, Ind), 5.49 (d, 5 Hz, 1H, Ind), 5.98 (s, 1H, Cp), 6.03 (s, 1H, Cp), 6.05 (s, 1H, Cp), 6.23 (s, 1H, Cp), 6.68−6.75 (br m, 3H, Ind), 6.79 (t, 10 Hz, 1H, Ind), 7.26 (d, 10 Hz, 1H, Ind), 7.37 (d, 10 Hz, 1H, Ind), 7.62 (d, 10 Hz, 1H, Ind), 7.69 (d, 10 Hz, 1H, Ind). $^{13}$C NMR (toluene-$d_8$, -34 °C): $\delta$ = 1.53 (Si$Me_3$), 1.86 (Si$Me_3$), 2.36 (Si$Me_3$), 2.55 (Si$Me_3$), 30.28 (*C*Me$_3$), 33.14 (C$Me_3$), 33.17 (C$Me_3$), 33.48 (*C*Me$_3$), 33.72 (*C*Me$_3$), 34.29 (*C*Me$_3$), 34.46 (C$Me_3$), 34.90 (C$Me_3$), 71.29, 72.66, 73.25, 75.19, 93.58, 93.86, 95.24, 95.95, 96.19, 106.77, 112.09, 112.61 (Cp), 122.07, 122.27, 122.62, 122.69, 122.90, 123.76, 123.95, 124.54, 124.86, 125.05, 125.85, 126.09, 126.27, 126.59, 126.69, 126.74, 127.07, 128.69, 129.62, 136.55, 137.02, 137.62 (Ind). Two Ind resonances not located.

**Preparation of ($\eta^5$-$C_9H_5$-1,3-($CHMe_2$)$_2$)($\eta^9$-$C_9H_5$-1,3-($CHMe_2$)$_2$)-Zr (5).** A 100 mL round-bottomed flask was charged with 26.29 g (0.131 mmol) of mercury and approximately 10 mL of toluene. While stirring, 0.132 g (5.72 mmol) of sodium metal was added and the resulting amalgam was stirred for an additional 20 min. A toluene slurry containing 0.535 g (0.954 mmol) of **5-Cl$_2$** was added. The resulting reaction mixture was stirred vigorously for 2 days, and the purple solution was decanted from the amalgam and filtered through Celite. Removal of the toluene in vacuo followed by recrystallization from pentane at −35 °C afforded 0.336 g (72%) of **5** as a burgundy solid. Anal. Calcd for $C_{30}H_{38}Zr$: C, 73.56; H, 7.82. Found: C, 73.45; H, 8.08. $^1$H NMR (toluene-$d_8$, −34 °C): $\delta$ = 1.07 (d, 3 Hz, 6H, CH(C$H_3$)$_2$), 1.10 (d, 3 Hz, 6H, CH(C$H_3$)$_2$), 1.14 (d, 3 Hz, 6H, CH(C$H_3$)$_2$), 1.18 (d, 3 Hz, 6H, CH(C$H_3$)$_2$), 2.58 (sept, 3 Hz, 2H, C*H*(CH$_3$)$_2$), 2.99 (sept, 3 Hz, 2H, C*H*(CH$_3$)$_2$), 3.65 (br s, 2H, Ind), 4.84 (br s, 2H, Ind), 5.83 (s, 1H, Cp), 6.62 (s, 1H, Cp), 6.85 (br s, 2H, Ind), 7.17 (br s, 2H, Ind). $^{13}$C NMR (toluene-$d_8$, −34 °C): $\delta$ = 22.26, 22.30, 26.34, 27.20, 27.62, 29.44 (CH(CH$_3$)$_2$), 69.41, 96.98 (Ind), 102.49, 115.31, 116.02, 120.98, 121.02, 121.27, 123.69, 127.85 (Cp/Ind).

**Preparation of ($\eta^5$-$C_9H_5$-1,3-($SiMe_3$)$_2$)($\eta^9$-$C_9H_5$-1,3-($SiMe_2Ph$)$_2$))-Zr (6).** This molecule was synthesized using a procedure similar to that described for **2** with 0.654 g (0.81 mmol) of **6-Cl$_2$** and 0.104 g (1.62 mmol) of $LiCH_2CHMe_2$, yielding 0.129 g (22%) of burgundy solid **6** as an equimolar mixture of isomers. Anal. Calcd for $C_{40}H_{50}Si_4Zr$: C, 65.42; H, 6.86. Found: C, 65.41; H, 7.06. $^1$H NMR (toluene-$d_8$, −34 °C): $\delta$ = 0.22 (s, 18H, Si$Me_3$), 0.33 (s, 18H, Si$Me_3$), 0.42 (s, 6H, Si$Me_2$Ph), 0.50 (s, 6H, Si$Me_2$Ph), 0.66 (s, 6H, Si$Me_2$Ph), 0.72 (s, 6H, Si$Me_2$Ph), 3.82 (br s, 2H, Ind), 3.90 (br s, 2H, Ind), 5.35 (br s, 2H, Ind), 5.41 (br s, 2H, Ind), 5.35 (s, 1H, Cp), 5.41 (s, 1H, Cp), 6.19 (s, 1H, Cp), 6.23 (s, 1H, Cp), 6.67 (m, 2H, Ind), 6.82 (m, 2H, Ind), 7.33 (m, 10H, Ph), 7.40 (m, 10H, Ph), 7.45 (m, 2H, Ind), 7.48 (m, 2H, Ind). $^{13}$C NMR (toluene-$d_8$, −34 °C): $\delta$ = −0.38 (Si$Me_2$Ph), −0.14 (Si$Me_2$Ph), 1.03 (Si$Me_2$Ph), 1.46 (Si$Me_3$), 2.32 (Si$Me_3$), 74.88, 75.24, 95.03, 95.23 (Ind), 99.97, 102.98, 109.95, 112.45, 118.78, 120.29, 123.50, 123.72 (Cp), 126.85, 131.55, 131.80, 133.11, 133.47, 134.47, 134.62, 134.72, 134.89, 136.51, 138.52, 140.31, 140.35 (Ind/Ph). One SiMe$_2$Ph and three Ind/Ph resonances not located.

**Preparation of ($\eta^5$-$C_9H_5$-1,3-($SiMe_3$)$_2$)($\eta^9$-$C_9H_5$-1-($SiMe_3$)-3-($CMe_3$))-Zr (7).** This molecule was prepared in an identical manner to **2** with 0.769 g (1.16 mmol) of **7-Cl$_2$** and 0.149 g (2.33 mmol) of $LiCH_2CHMe_2$, yielding 0.282 g (41%) of a burgundy solid identified as **7**. Anal. Calcd for $C_{31}H_{46}Si_3Zr$: C, 62.66; H, 7.80. Found: C, 62.16; H, 7.52. $^1$H NMR (benzene-$d_6$): $\delta$ = 0.23 (s, 9H, Si$Me_3$), 0.28 (s, 9H, Si$Me_3$), 0.34 (s, 9H, Si$Me_3$), 1.28 (s, 9H, C$Me_3$), 3.82 (t, 3 Hz, 1H, Ind), 4.07 (t, 3 Hz, 1H, Ind), 5.15 (d, 3 Hz, 1H, Ind), 5.46 (d, 3 Hz, 1H, Ind), 6.09 (s, 1H, Cp), 6.40 (s, 1H, Cp), 6.79 (br s, 2H, Ind), 7.46 (d, 5 Hz, 1H, Ind), 7.60 (d, 5 Hz, 1H, Ind). $^{13}$C NMR (benzene-$d_6$): $\delta$ = 1.08 (Si$Me_3$), 1.29 (Si$Me_3$), 2.20 (Si$Me_3$), 33.73 (*C*Me$_3$), 34.27 (C$Me_3$), 71.81, 74.05, 93.10, 94.89 (Ind), 102.86, 105.96, 108.31, 119.19, 122.70, 122.78, 122.91, 126.16, 126.50, 126.85, 128.03, 131.18, 131.46, 136.69 (Cp/Ind).

**Preparation of ($\eta^5$-$C_9H_5$-1,3-($SiMe_3$)$_2$)$_2$Zr($\eta^5$-$CH_2C(Me)CH_2$)H (5-($\eta^3$-$CH_2C(Me)CH_2$)H).** A 25 mL round-bottomed flask was charged with 0.105 g (0.214 mmol) of **5** and dissolved in 5 mL of pentane in a drybox. A 180° needle valve was attached, and the reaction was degassed before 625 Torr (1.07 mmol) of isobutylene was added by a calibrated gas bulb. The reaction was stirred overnight before solvent was removed in vacuo. Extraction with pentane followed by filtration through a 1 mL frit and solvent removal in vacuo gave a foamy red solid. Recrystallization from pentane at −35 °C afforded 0.042 g (36%) of **5-($\eta^3$-$CH_2C(Me)CH_2$)H** as a red solid. Anal. Calcd for $C_{42}H_{70}Si_4Zr$: C, 74.80; H, 8.49. Found: C, 74.36; H, 8.30. $^1$H NMR (toluene-$d_8$, −38 °C): $\delta$ = −2.66 (s, 1H, C$H_2$CMeCH$_2$), 1.06 (d, 8 Hz, 3H, CH(C$H_3$)$_2$), 1.09 (d, 8 Hz, 3H, CH(C$H_3$)$_2$), 1.21 (m, 6H, CH(C$H_3$)$_2$), 1.21 (s, 1H, CH$_2$CMeC$H_2$), 1.30 (d, 8 Hz, 3H, CH(C$H_3$)$_2$), 1.34 (d, 8 Hz, 3H, CH(C$H_3$)$_2$), 1.44 (s, 3H, CH$_2$C*Me*CH$_2$), 1.77 (d, 8 Hz, 3H, CH(C$H_3$)$_2$), 2.18 (d, 8 Hz, 3H, CH(C$H_3$)$_2$), 2.48 (s, 1H, Zr-*H*), 2.76 (m, 1H, C*H*(CH$_3$)$_2$), 2.78 (s, 1H, Cp), 2.87 (m, 1H, C*H*(CH$_3$)$_2$), 2.90 (s, 1H, CH$_2$CMeC$H_2$), 3.20 (m, 1H, C*H*(CH$_3$)$_2$), 3.59 (s, 1H, Cp), 3.92 (s, 1H, C$H_2$CMeCH$_2$), 3.99 (m, 1H, C*H*(CH$_3$)$_2$), 6.57 (m, 1H, Ind), 6.65 (m, 1H, Ind), 6.87 (br s, 3H, Ind), 7.51 (m, 1H, Ind), 7.57 (br s, 2H, Ind). $^{13}$C NMR (toluene-$d_8$, −38 °C): $\delta$ = 22.59, 23.46, 24.25, 25.04, 25.89, 26.41, 26.84, 27.03 (CH(CH$_3$)$_2$), 28.21 (CH$_2$C*Me*CH$_2$), 28.73, 29.33, 29.67, 31.88, 35.00 (CH(CH$_3$)$_2$), 58.19 (*C*H$_2$CMeCH$_2$), 70.66 (CH$_2$CMe*C*H$_2$), 105.89 (Cp), 111.25 (Cp/Ind), 112.67 (Cp/Ind),

112.81 (Cp), 115.65, 117.32, 118.91, 120.47, 121.69, 121.83, 121.98, 122.18, 122.58, 123.17, 134.10 (Cp/Ind). Three Cp/Ind resonances not located.

**Preparation of ($\eta^5$-$C_9H_5$-1,3-$(CHMe_2)_2$)$_2$Zr($\eta^3$-$CH_2CHC(Me)H$)-H (5-($\eta^3$-$CH_2C(Me)CH_2$)H).** This molecule was prepared in an similar manner as **5-($\eta^5$-$CH_2C(Me)CH_2$)H** with 0.015 g (0.031 mmol) of **5** and 18 Torr (0.30 mmol) of 1-butene. $^1$H NMR (toluene-$d_8$, −38 °C): $\delta$ = −1.01 (d, 10 Hz, 1H, C*H*$_2$CHCHCH$_3$), 1.18 (m, 1H, CH$_2$-CHC*H*CH$_3$), 1.23 (d, 8 Hz, 3H, CH(C*H*$_3$)$_2$), 1.25 (d, 8 Hz, 3H, CH-(C*H*$_3$)$_2$), 1.29 (d, 8 Hz, 3H, CH(C*H*$_3$)$_2$), 1.38 (d, 8 Hz, 3H, CH(C*H*$_3$)$_2$), 1.43 (d, 8 Hz, 3H, CH(C*H*$_3$)$_2$), 1.46 (d, 8 Hz, 3H, CH(C*H*$_3$)$_2$), 1.56 (d, 8 Hz, 3H, CH(C*H*$_3$)$_2$), 1.60 (d, 8 Hz, 3H, CH(C*H*$_3$)$_2$), 1.80 (d, 10 Hz, 1H, C*H*$_2$CHCHCH$_3$), 2.02 (br s, 1H, CH$_2$C*H*CHCH$_3$), 2.17 (br s, 3H, CH$_2$CHCHC*H*$_3$), 3.07 (m, 1H, C*H*(CH$_3$)$_2$), 3.23 (m, 2H, C*H*(CH$_3$)$_2$ and Zr-*H*), 3.45 (m, 2H, C*H*(CH$_3$)$_2$), 4.51 (s, 1H, Cp), 4.95 (s, 1H, Cp), 6.54 (m, 1H, Ind), 6.64 (m, 1H, Ind), 6.68 (m, 1H, Ind), 6.77 (m, 1H, Ind), 6.98 (d, 12 Hz, 1H, Ind), 7.05 (d, 12 Hz, 1H, Ind), 7.20 (d, 12 Hz, 1H, Ind), 7.39 (d, 12 Hz, 1H, Ind). $^{13}$C NMR (toluene-$d_8$, −38 °C): $\delta$ = 13.67, 21.58, 22.90, 23.92, 25.23, 25.35, 25.63, 26.22, 26.40, 27.58, 28.28, 28.49, 29.00, 29.45, 30.16, 52.57 (CH(CH$_3$)$_2$/CH$_2$-CHCHCH$_3$), 95.10, 105.05, 115.54, 116.81, 117.53, 118.03, 118.34, 120.50, 120.80, 121.39, 121.68, 121.79, 122.15, 122.77, 123.28, 123.51, 123.69, 125.06 (Cp/Ind).

**Acknowledgment.** We thank the Cornell University Department of Chemistry and Chemical Biology, the donors of the Petroleum Research Fund administered by the American Chemical Society, and the National Science Foundation (predoctoral fellowship to C.A.B. and CAREER Award to P.J.C.) for generous financial support. P.J.C. is also a Cottrell Scholar and acknowledges financial support from the Research Corporation.

**Supporting Information Available:** Additional experimental procedures, NMR spectroscopic data, computational results, and crystallographic data for **3**, **5**, and **5-($\eta^3$-$CH_2C(Me)CH_2$)H** including full atom labeling schemes and complete bond distances and angles (PDF, CIF). This material is available free of charge via the Internet at http://pubs.acs.org.

JA045072V